

# **MULTIPLE-RESONATOR MAGNETIC RESONANT COUPLING WIRELESS POWER TRANSFER**

by

**Hao Wang**

B.S. in Engineering, Tsinghua University, China, 2009

Submitted to the Graduate Faculty of  
the Swanson School of Engineering in partial fulfillment  
of the requirements for the degree of  
**Master of Science**

University of Pittsburgh

2011

UNIVERSITY OF PITTSBURGH  
SWANSON SCHOOL OF ENGINEERING

This thesis was presented

by

Hao Wang

It was defended on

November 30, 2011

and approved by

Mingui Sun, Ph.D., Professor, Departments of Neurological surgery, BioEngineering and

Electrical and Computer Engineering

Marlin H. Mickle, Ph.D., Nickolas A. DeCecco Professor; Professor, Departments of

Electrical and Computer Engineering, Telecommunications and Industrial Engineering;

Executive Director, RFID Center of Excellence

Robert J. Sclabassi, Ph.D., Professor Emeritus, Computational Diagnostics Inc.

Zhi-Hong Mao, Ph.D., Associate Professor, Departments of Electrical and Computer

Engineering and BioEngineering

Thesis Advisor: Mingui Sun, Ph.D., Professor, Departments of Neurological surgery,

BioEngineering and Electrical and Computer Engineering



Copyright © by Hao Wang  
2011

# **MULTIPLE-RESONATOR MAGNETIC RESONANT COUPLING WIRELESS POWER TRANSFER**

Hao Wang, M.S.

University of Pittsburgh, 2011

With the developments of mobile and implantable devices, wireless power transfer (WPT) has become increasingly necessary to free a variety of electronic systems from using power cords and batteries. WPT is especially important in providing medical implants with an alternative power source since changing battery in an implant implies a surgery. In recent years, several WPT methods have emerged, including magnetic induction and omnidirectional or unidirectional electromagnetic radiation. In 2007, a magnetic resonant coupling WPT method was reported which brought the research on WPT to a new climax. This new method transmits power wirelessly in the mid-range, which represents several times the average radius of the resonators in the WPT system. The energy transmission efficiency of the new method is much higher than the magnetic induction method. In addition, the new method does not suffer from the tracking problem as the unidirectional electromagnetic radiation method does. Despite the advantages, a simple two-resonator WPT system has limited applications due to the insufficient transmission range in many practical applications. A multiple-resonator system provides an effective solution to this problem, but has not yet been fully understood despite the recent interest in this subject. In this thesis, the three-resonator relayed WPT system is analyzed theoretically. The coupled mode theory (CMT) is utilized to find the optimal relay position at which the maximum efficiency is achieved. Experiments were performed which verified the results of our theoretical analysis. It was found that the relay resonator increased the WPT distance significantly while providing a high energy transfer efficiency. As an important application, we constructed a new plat-

form for performing biological experiments on laboratory rodents implanted with miniature devices. Our WPT system supplies a sufficient amount energy to the implanted devices regardless of the locations of rodents in the platform. A new hexagonal PCB based resonator was designed. Seven such resonators were fabricated and placed under the platform in a unique pattern. These resonators transmit power to an innovative receiving resonator which is integrated within the container of an implanted device.

**Keywords:** Resonant, Coupling, Wireless, Coupled Mode Theory, Multiple-resonator.

## TABLE OF CONTENTS

<b>1.0 INTRODUCTION</b>	1
1.1 background and motivation	1
1.2 thesis outline	8
<b>2.0 LITERATURE REVIEW</b>	9
2.1 review of coupled mode theory	10
2.2 brief review of equivalent circuit method	17
2.3 comparing CMT and EQC methods	19
<b>3.0 METHODS</b>	20
3.1 theoretical analysis	20
3.2 experiments	23
3.2.1 RESONATOR DESIGN	23
3.2.2 PARAMETER MEASUREMENT	24
3.2.2.1 SOURCE LOOP MANUFACTURING	24
3.2.2.2 NATURAL FREQUENCY, Q FACTOR AND COUPLING CO-EFFICIENT MEASUREMENT	26
3.2.3 EFFICIENCY MEASUREMENT	28
3.3 Applications	31
3.3.1 MULTIPLE-RESONATOR TRANSMITTER DESIGN	32
3.3.2 RECEIVING RESONATOR DESIGN	32
3.3.3 POWER TRANSFER MEASUREMENT	32
<b>4.0 RESULTS AND DISCUSSIONS</b>	37
4.1 relayed WPT system	37

4.2 multiple-coil-transmitter powering platform . . . . .	41
<b>5.0 CONCLUSIONS AND CONTRIBUTIONS . . . . .</b>	<b>43</b>
5.1 contributions . . . . .	43
5.2 future work . . . . .	44
<b>BIBLIOGRAPHY . . . . .</b>	<b>45</b>

## LIST OF TABLES

1	Resonant frequency, Q factor and Intrinsic loss . . . . .	37
2	$\kappa$ vs distance . . . . .	38
3	Statistical features of measured induced voltage . . . . .	42

## LIST OF FIGURES

1	Nikola Tesla photo by Sarony of New York . . . . .	2
2	Tesla Tower . . . . .	3
3	Sketch of a radiative WPT system . . . . .	3
4	SSPS system [1] . . . . .	4
5	Sketch of a magnetic induction WPT system. . . . .	6
6	A wireless cell phone charging system [2] . . . . .	6
7	Sketch of a two-resonator witricity system . . . . .	7
8	A car charging system based on witricity [3] . . . . .	7
9	LC circuit . . . . .	11
10	RLC circuit . . . . .	13
11	Equivalent circuit of a two-resonator magnetic resonant coupling WPT system	17
12	Witricity system with relay. . . . .	20
13	Self-resonant coil used in the experiment. . . . .	24
14	Source loop. . . . .	25
15	Experimental setup to measure Q factor. . . . .	26
16	$S_{11}$ curve in smith chart and 45-degree method to measure Q factor. . . . .	27
17	Experimental setup to measure coupling coefficients. . . . .	29
18	SWR curve of a two-resonator system and frequency splitting method to measure coupling coefficient. . . . .	30
19	Experimental setup for efficiency measurement . . . . .	31
20	7-resonator transmitter . . . . .	33
21	driving loops for multiple-resonator transomitter . . . . .	34

22	New receiving resonator . . . . .	34
23	Experimental setup for measuring induced voltage . . . . .	35
24	Receiving resonator positions for induced voltage measurement . . . . .	36
25	$\kappa$ vs. distance . . . . .	39
26	Efficiency vs. distance between S and R. . . . .	40
27	Induced voltage measurement result . . . . .	42



## 1.0 INTRODUCTION

### 1.1 BACKGROUND AND MOTIVATION

The idea of transmitting electromagnetic power wirelessly traces back to over one hundred years ago, when Nikola Tesla, one of the most brilliant inventors in the 19th and 20th century, came up with the innovative power distribution method and got his patent "apparatus for transmitting electrical energy" in 1914 [4]. He even built a huge transmission tower on Long Island, but unfortunately this project was aborted due to some financial problem [5]. Because of the great success of power grid, wireless energy transmission came to low ebb and hadn't had much progress for a long time. Now with the development of wireless communication and mobile devices, an age of wirelessness has come. But people still need wire to recharge those devices, so the call for wireless energy transmission is becoming louder and louder. Besides, in some situations where it is either difficult or dangerous to change batteries for devices, wireless power transmission is also needed badly, such as for implanted devices in human body. In this situation, several wireless power transmission (WPT) technologies were developed and came into our lives, among which the most important three are radiative method, magnetic induction method and magnetic resonant coupling method.

Radiative method is a well-developed long distance wireless power transmission method, where microwave is usually used to transmit energy. Basically, energy, in the form of microwave, is transmitted between the source and device antennas, just like what is happening in the wireless communication. Many applications have been developed based on the radiative method, and one of the most famous one would be the space satellite power system (SSPS). Back in the 1960's a paper talked about the sun power started the research about the SSPS [6], where people used solar panel to gather solar power in the space and microwave is

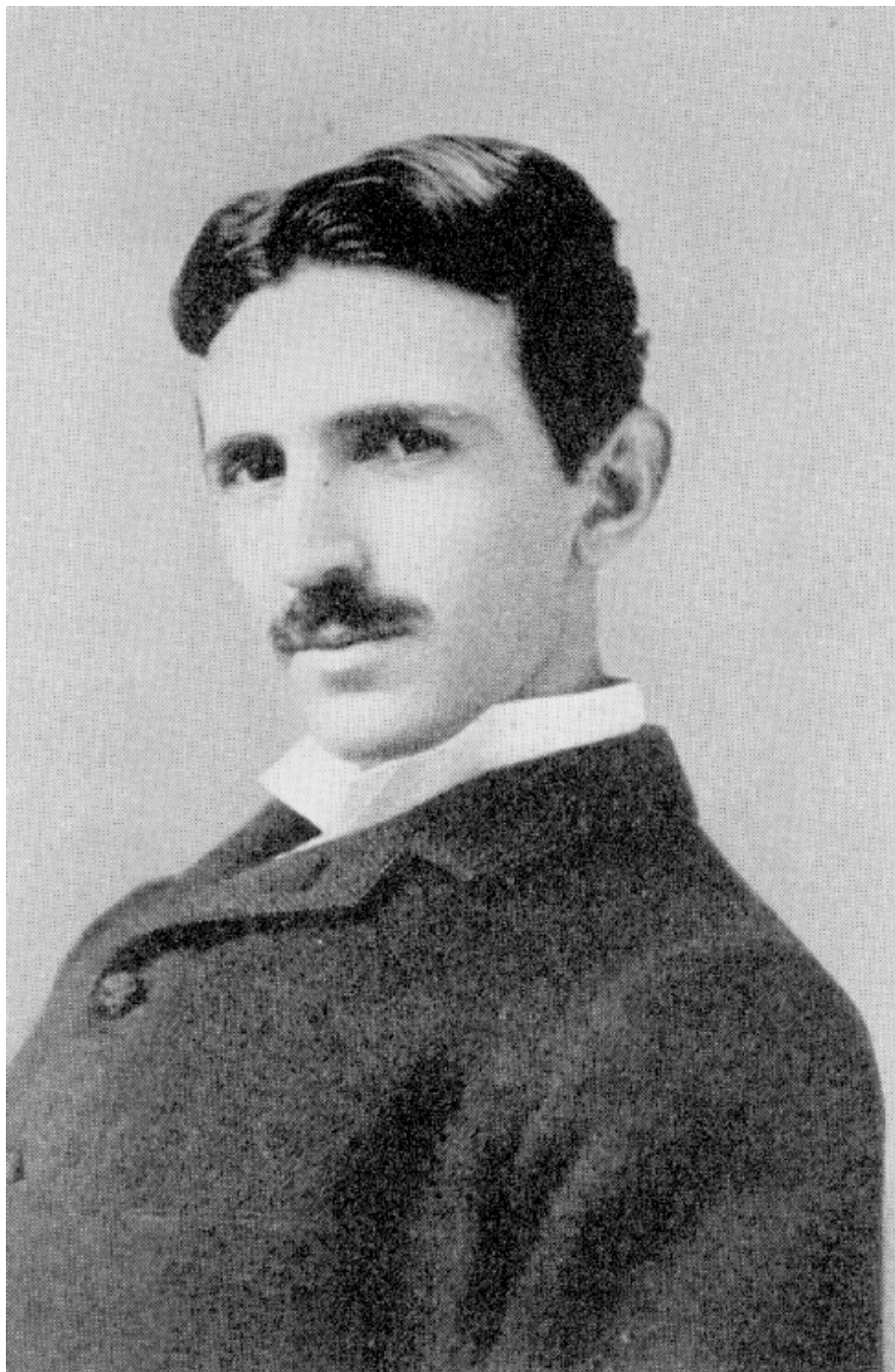


Figure 1: Nikola Tesla photo by Sarony of New York



Figure 2: Tesla Tower

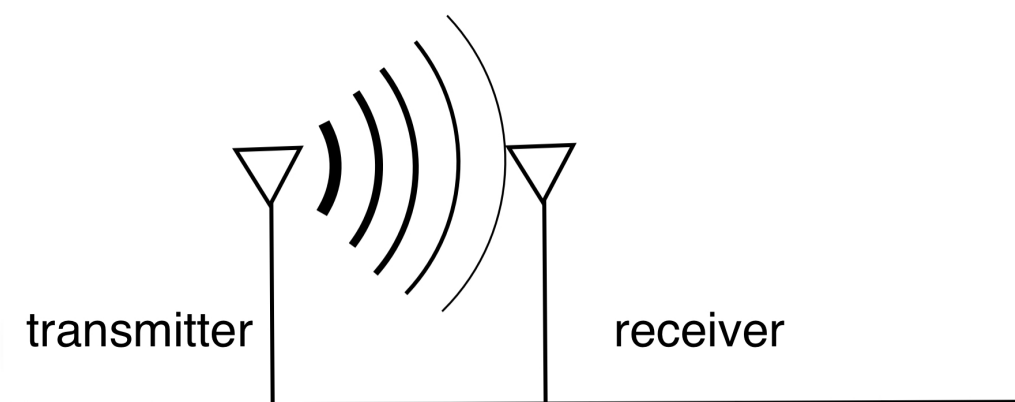


Figure 3: Sketch of a radiative WPT system



Figure 4: SSPS system [1]

used to transfer energy back to earth. This is probably the largest man-made wireless power transmission system. Despite the long transmission distance, the radiative method, however, suffers from several major problems. Intuitively, an omnidirectional antenna can not give us a high efficiency, because most of the energy is sent to other directions and wasted. So to enhance the efficiency, the transmitter antenna must be highly directional. Using this kind of directional antenna, NASA achieved 82.5% efficiency at one-mile distance in 1975 [7]. In this case, how to develop a highly directional antenna is a critical problem that people have been trying to solve and made much progress [8]. However, this highly directional antenna will cause another problem, which is that a tracking system is needed to power a moving object, and this tracking system will make the whole WPT system much more complex. Another problem for the radiative method is that the transmission can be blocked easily, so no obstacles can be placed between the transmitter and the receiver [9].

The magnetic induction method was developed directly based on the Faraday's law of electromagnetic induction, which was discovered by Faraday in 1831 [10]. The whole magnetic induction WPT system consists two coils, namely transmitting and receiving coils. These two coils are strongly coupled so that the current change in the transmitting coil could generate voltage in the receiving coil and thus energy is transferred from transmitting coil to receiving coil. Now many products are invented using magnetic induction wireless power transfer, including electronic tooth brush and wireless cell phone charging system and etc. The magnetic induction method could get high efficiency in near field, but the efficiency decreases quickly as the distance between the transmitting coil and receiving coil increases, and thus is only feasible for power transmission over several centimeters [11, 12].

In 2007, a group in MIT came up with an innovative WPT method, known as witrlicity [13, 9]. Strongly coupled magnetic resonators are used in this method, so this method is also known as magnetic resonant coupling method. This method is similar to the near field method, where two coils couple with each other directly through magnetic field, however, here the two coils are replaced with two magnetic resonators. The introducing of resonant coupling increases the power transfer range from short range to mid-range, which can be several times the average radius of the resonators, and the increase of power transfer range in turn increases the number of applications that can apply this technology. The magnetic

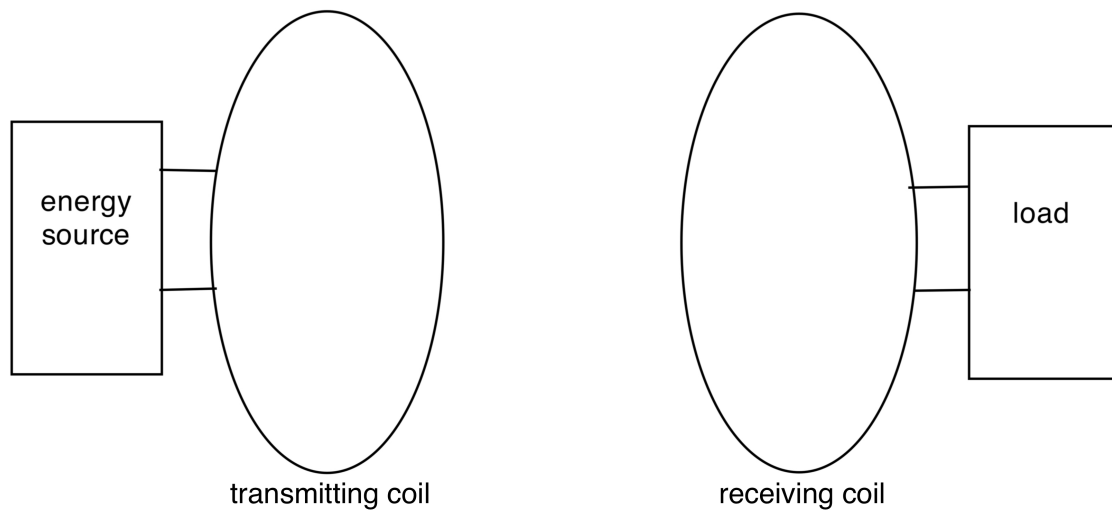


Figure 5: Sketch of a magnetic induction WPT system.



Figure 6: A wireless cell phone charging system [2]

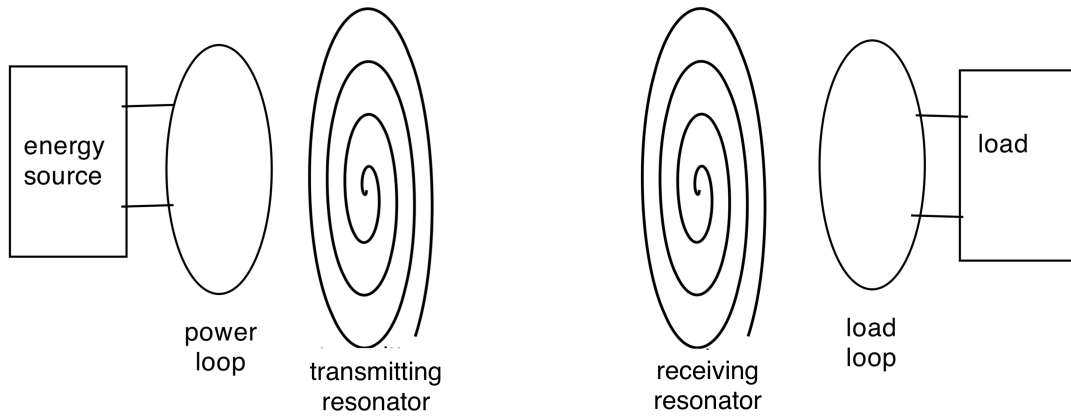


Figure 7: Sketch of a two-resonator witrlicity system

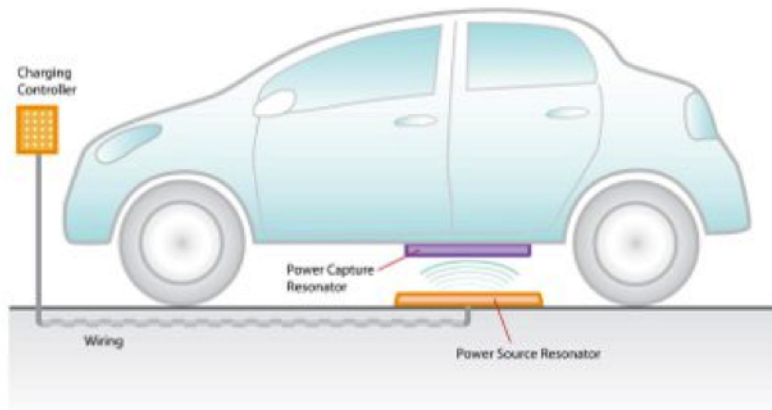


Figure 8: A car charging system based on witrlicity [\[3\]](#)

resonant coupling method has no tracking or blocking problem as for radiative method and can get high efficiency at a much longer distance than the magnetic induction method could. The research on the magnetic resonant coupling method is increasing rapidly, and in this paper, the author will focus on this mid-range method, and more specifically, the magnetic resonant coupling WPT method with multiple ( $>2$ ) resonators.

## 1.2 THESIS OUTLINE

This thesis is divided into 5 chapters: Chapter 2 is a review of the recent work on resonant coupled WPT system and also an introduction to the two major methods, namely Coupled Mode Theory (CMT) and Equivalent Circuit Method (EQC). Chapter 3 outlines the theoretical analysis together with the experimental verification of a relayed resonant coupled WPT system. Also, an new platform for performing biological experiments on laboratory rodents implanted with miniature devices is discussed in this chapter as an application of multiple-resonator WPT system. Chapter 4 shows the experimental results and a discussion about the experimental and theoretical results. The conclusion is presented in Chapter 5.



## 2.0 LITERATURE REVIEW

Many researches have been done on the magnetic resonant coupling WPT system since 2007, most of which use two methods to analyze this system namely the coupled mode theory (CMT), which has been a handy tool to analyze resonators since 1950's, and the equivalent circuit method (EQC). Karalis et al developed the two-resonator witricity system based on the CMT method, the optimal coupling coefficient and load were found in terms of resonator parameters to get the maximum efficiency [13, 9]. In 2009, Benjamin, James and Seth studied the WPT system to power multiple small receiving resonators [14]. This research is based on the circuit theory, and the small receiving resonators are placed far from each other so the coupling between the receiving resonators can be ignored. The voltage gain from source to load is evaluated and tested. Andre et al also published a paper about powering multiple devices in 2010 [15]. CMT theory was used in this research, however because of the complexity of matrix inversion, the number of devices is restricted to 2, and to further simplify this model, the receiving resonators are much smaller than the transmitting resonator and are placed on different sides of the transmitting resonator symmetrically so that the coupling of the two receiving resonators can be ignored. The result shows that the total efficiency of the three-resonator system is higher than that of a two-resonator system. In 2010, Jin-Wook et al studied the power deliver to multiple devices also based on the CMT theory [16]. In their research, the receiving resonators were placed in such a form that the adjacent resonators were perpendicular to each other so that the coupling of receiving resonators can be ignored. The ratio between energy stored in receiving resonators and energy stored in the whole system was tested and simulated, the result shows that this ratio increases when we increase the number of devices. Alanson, David and Joshua presented their work on mid-range power transfer system using the circuit theory in 2010 [17]. In their paper,

S parameter was introduced to the analysis of the system and was simulated with respect to different coupling coefficients and driving frequencies, also the idea of frequency tuning is introduced in this paper to make sure that the system is driven at optimal frequency. In the same year, Yong-Hae et al expanded the idea of frequency tuning to multiple-receiver systems and improved the performance of multiple-resonator WPT system [18]. Not only frequency tuning, impedance matching was also considered to improve the efficiency of witrlicity systems [19]. Fei et al. raised the relay problem about this WPT system in 2010 [20]. The response of each resonator was calculated using CMT theory and experiments were performed to find the optimal relay position so that the maximum efficiency can be achieved. Result shows that the relayed system can get much higher efficiency than the original system and the optimal relay position is around the midpoint between the transmitting and receiving resonators. Other than the CMT and EQC method, many researches have also been done using other approaches. In 2011, Marco and Mauro attacked the system using network theory [21]. Hiroshi et al investigated the calculation of system parameters from electrodynamics and the effect of system parameters to system performance [22]. Power loss factors were evaluated numerically by Satoshi et al [23]. Hyeon-Chang et al studied the resonator design problem to maximize the efficiency [24]. Takehiro et al brought in the problem of maximizing transmission distances [25].

Because CMT and EQC are the most commonly used tools to analyze a magnetic resonant coupling WPT system, they will be introduced in the next two sections.

## 2.1 REVIEW OF COUPLED MODE THEORY

In the 1950's, Miller and Pierce developed the CMT to study the microwave transmission lines and electron beams problem. This theory was then generalized to analyze a large number of problems in microwave waveguide and optoelectronic area. There are many possible modes in a RF device, for example a microwave waveguide, and the CMT is to analyze a coupled system by handling the modes of the uncoupled system. Schelkunoff gave a rigorous derivation of CMT, showing that if a complete set of modes is used, the CMT is equivalent

to Maxwell's equations. However, in most cases, only the first one or two modes are used, so the CMT is still an approximation [26]. In the case of magnetic resonant coupling WPT, only the lowest order modes are considered, which are the natural frequencies of those resonators. In this section, the CMT is introduced in detail. Figure 9 shows an LC circuit, which is the basic component of a resonant system. Here the voltage on the capacitor and the current

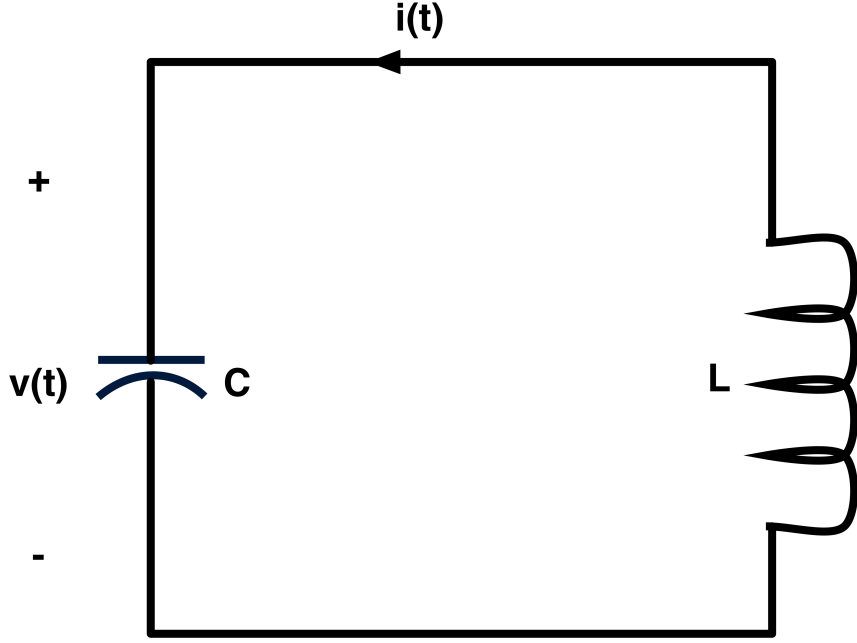


Figure 9: LC circuit

across the inductor are selected as the state variable to describe the circuit and we can write the following state equations:

$$\begin{aligned} \dot{i} &= C \frac{dv}{dt} \\ v &= -L \frac{di}{dt}. \end{aligned} \tag{2.1}$$

To simplify the analyze, a decoupling is performed and the decoupled variables can be calculated as:

$$a_{\pm} = \sqrt{\frac{C}{2}}v \pm j\sqrt{\frac{L}{2}}i. \tag{2.2}$$

This way, the new state equations are:

$$\begin{aligned}\dot{a}_+ &= j\omega_0 a_+ \\ \dot{a}_- &= -j\omega_0 a_- \end{aligned} \tag{2.3}$$

where  $\omega_0 = \frac{1}{\sqrt{LC}}$  is the natural frequency of the resonator,  $a_+$  and  $a_-$  are known as positive and negative frequency components respectively. As shown in (2.3), these two equations are complex conjugations of each other, so one of them is enough to totally describe the system, and the author chose to use the equation of  $a_+$ , and will denote  $a_+$  as  $a$  from now on. Another important property of these frequency components is that  $|a_{\pm}|^2$  equals the energy stored in the resonator. This can be shown by directly solve (2.1), and the solution is:

$$\begin{aligned}v &= V \sin(\omega_0 t + \theta) \\ i &= CV\omega_0 \cos(\omega_0 t + \theta). \end{aligned} \tag{2.4}$$

Plugging (2.4) into the definition of  $a_+$ , we get

$$a = \sqrt{\frac{C}{2}} V \sin(\omega_0 t + \theta) + j \sqrt{\frac{C}{2}} V \cos(\omega_0 t + \theta) = \sqrt{\frac{C}{2}} V e^{j(\omega_0 t + \theta)}. \tag{2.5}$$

So

$$|a|^2 = \frac{C}{2} V^2 = E. \tag{2.6}$$

Until now we have been talking about lossless resonators, and if there is loss, the state equation can be modified to

$$\dot{a} = j\omega_0 a - \Gamma_0 a. \tag{2.7}$$

This is an approximation when the loss is small. To see this more clearly, we look at an RLC circuit, which is shown in Figure 10. The state equations for this RLC circuit is

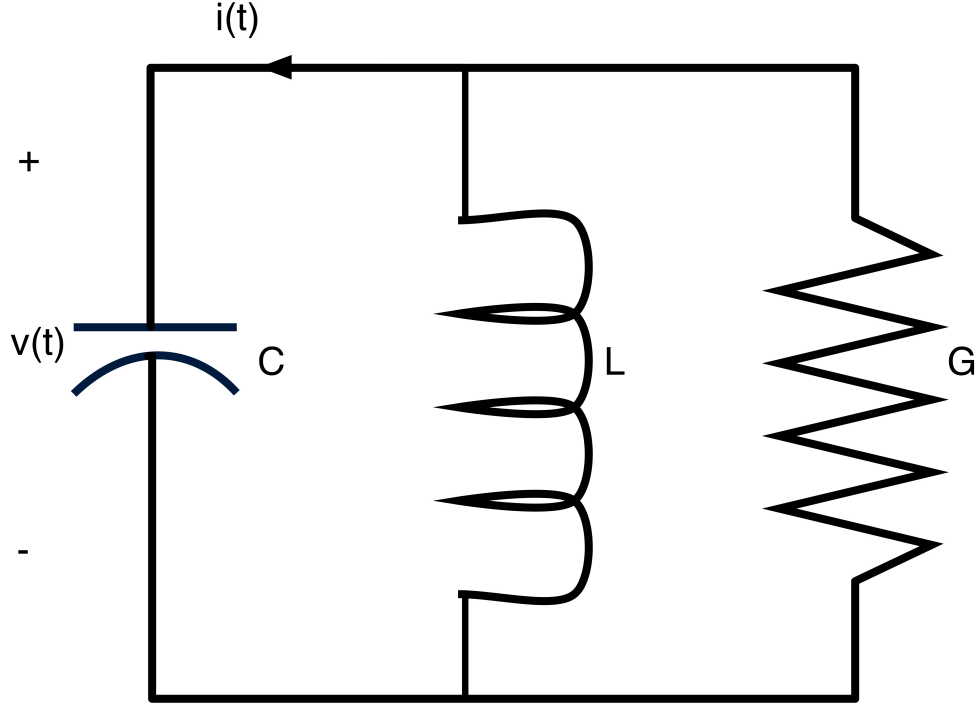


Figure 10: RLC circuit

$$\begin{aligned} i &= C \frac{dv}{dt} + Gv \\ v &= -L \frac{di}{dt}. \end{aligned} \quad (2.8)$$

Calculating the complex frequency of this system, we get

$$s = j\omega - \Gamma = j \sqrt{\frac{1}{LC} - \frac{G^2}{4C^2}} - \frac{G}{2C}. \quad (2.9)$$

When the loss is small, which means  $G$  is small, the second term under the square root can be ignored, which gives us (2.7). This also shows that the coupled mode theory is more accurate for resonators with higher natural frequencies and higher  $Q$  factors.

Now we look into the power loss in more details. From physical meaning, the power loss  $P_L$  is

$$P_L = -\frac{dE}{dt} = -\frac{d|a|^2}{dt} = -a \frac{da^*}{dt} - a^* \frac{da}{dt} = 2\Gamma_0 |a|^2 = 2\Gamma_0 E. \quad (2.10)$$

So the Q factor can be calculated as

$$Q = \frac{\omega_0 E}{P_L} = \frac{\omega_0}{2\Gamma_0}. \quad (2.11)$$

This equation is important for calculating  $\Gamma_0$  in experiments, as Q factor and natural frequency can be measured using network analyzer.

Now we are getting into the coupling between resonators and will start from the easiest case, two resonators, namely resonator 1 and 2 with the positive frequency components  $a_1$  and  $a_2$  and we consider them lossless. The differential equations for this system is

$$\begin{aligned} \dot{a}_1 &= j\omega_1 a_1 + j\kappa_{12} a_2 \\ \dot{a}_2 &= j\omega_2 a_2 + j\kappa_{21} a_1 \end{aligned} \quad (2.12)$$

where  $\kappa_{12}$  and  $\kappa_{21}$  are known as coupling coefficients.

(2.12) is similar to what we found in one resonator case except for those coupling terms. People may expect the  $\kappa$ 's to be liner integrodifferential operators, however in the situation when  $|\kappa_{12} a_2|$  is much smaller than  $|(j\omega_1 - \Gamma_1) a_1|$ , the coupling will affect the time evolution of  $a_1$  and  $a_2$  only when  $\omega_1$  is similar to  $\omega_2$ , in which case the time dependence is approximately in the form of  $e^{j\frac{\omega_1 + \omega_2}{2}t}$ , so both integral and differential operators are equivalent to multiplying a complex number [27].

$\kappa_{12}$  and  $\kappa_{21}$  are not independent due to the law of energy conservation, from which we have

$$\begin{aligned} \frac{d}{dt}(|a_1|^2 + |a_2|^2) &= j\kappa_{12} a_1^* a_2 - j\kappa_{12}^* a_2^* a_1 + j\kappa_{21} a_2^* a_1 - j\kappa_{21}^* a_1^* a_2 \\ &= (j\kappa_{12} - j\kappa_{21}^*) a_1^* a_2 + (j\kappa_{21} - j\kappa_{12}^*) a_1 a_2^* \\ &= 0. \end{aligned} \quad (2.13)$$

This in turn shows that

$$\kappa_{12} - \kappa_{21}^* = 0. \quad (2.14)$$

As  $\kappa$  totally depends on the resonant frequency and inductance of the resonators as shown in (2.15)

$$\kappa = \frac{\omega M}{\sqrt{L_1 L_2}} \quad (2.15)$$

where  $\omega$  is the resonant frequency,  $M$  is the mutual inductance of the two resonators and  $L_1$  and  $L_2$  are the self-inductances of the two resonators. So we can assert that  $\kappa_{12} = \kappa_{21} = \kappa$  is a real number.

Now we have set up the formula and explained all the parameters we need to analyze a magnetic resonant coupling WPT system, so in the next part a two-resonator witricity system will be taken as an example to show how to apply the CMT to analyze it.

A two-resonator witricity system has one transmitting resonator, which is inductively coupled with a source loop, and one receiving resonator, which is inductively coupled with a load loop, so the system setup is like what is shown in Figure 7. The differential equations describing the system can be written as

$$\begin{aligned}\dot{a}_{tr} &= (j\omega_0 - \Gamma_{tr})a_{tr} + j\kappa a_{re} + f \\ \dot{a}_{re} &= (j\omega_0 - \Gamma_{re} - \Gamma_w)a_{re} + j\kappa a_{tr}\end{aligned}\tag{2.16}$$

where  $a_{tr}$  and  $a_{re}$  are the positive frequency component in the transmitting resonator and receiving resonator respectively;  $\Gamma_{tr}$  and  $\Gamma_{re}$  are the intrinsic loss of each resonator and  $\Gamma_w$  is the load coupled with the receiving resonator;  $\kappa$  is the coupling coefficient between these two resonators, which is a real number; and  $f$  is the input coupled with the transmitting resonator.

Optimal conditions to get maximal efficiency are derived here to show the application of CMT on a WPT system. The physical definition of efficiency is the ratio of power on the load out of the total power supplied to the system, and this can be written as the following equation:

$$\eta = \frac{2\Gamma_w |a_{re}|^2}{2\Gamma_{tr} |a_{tr}|^2 + 2(\Gamma_w + \Gamma_{re}) |a_{re}|^2}.\tag{2.17}$$

The numerator is the power consumed on the load and the denominator is the total power consumption of the whole system, so the equation for efficiency is consistent with the physical definition. After some algebraic deduction, (2.17) becomes

$$\eta = \frac{\Gamma_w \frac{|a_{re}|^2}{|a_{tr}|^2}}{\Gamma_{tr} + (\Gamma_{re} + \Gamma_w) \frac{|a_{re}|^2}{|a_{tr}|^2}}.\tag{2.18}$$

(2.18) shows that  $\frac{|a_{re}|^2}{|a_{tr}|^2}$  is important to calculate the efficiency. This term can be found using (2.16). If we drive the system by a source with frequency  $\omega_0$ , in steady state both  $a_{tr}$  and  $a_{re}$  have a time-dependent term  $e^{j\omega_0 t}$ , then the second equation in (2.16) becomes

$$(\Gamma_{re} + \Gamma_w)a_{res} = j\kappa a_{trs} \quad (2.19)$$

where  $a_{res}$  and  $a_{trs}$  are the positive frequency components in steady state, so the steady state efficiency would be

$$\begin{aligned} \eta_s &= \frac{\Gamma_w \frac{|a_{res}|^2}{|a_{trs}|^2}}{\Gamma_{tr} + (\Gamma_w + \Gamma_{re}) \frac{|a_{res}|^2}{|a_{trs}|^2}} \\ &= \frac{\Gamma_w \kappa^2}{\Gamma_{tr}(\Gamma_w + \Gamma_{re})^2 + (\Gamma_w + \Gamma_{re})\kappa^2} \\ &= \frac{\frac{\Gamma_w}{\Gamma_{re}} \frac{\kappa^2}{\Gamma_{re}\Gamma_{tr}}}{(1 + \frac{\Gamma_w}{\Gamma_{re}})^2 + (1 + \frac{\Gamma_w}{\Gamma_{re}}) \frac{\kappa^2}{\Gamma_{re}\Gamma_{tr}}}. \end{aligned} \quad (2.20)$$

Now, to maximize the efficiency, we first set  $\frac{\partial \eta_s}{\partial \Gamma_w} = 0$ , and the optimal load we get is

$$\Gamma_{w,opt} = \sqrt{\Gamma_{re}^2 + \kappa^2 \frac{\Gamma_{re}}{\Gamma_{tr}}} \quad (2.21)$$

where  $\Gamma_{re}$ ,  $\Gamma_{tr}$  and  $\kappa^2$  are the parameters decided by the resonators and their relative position, so we consider them as constants for a given system. To prove that the obtained extremum is a maximum, we inspecting (2.20), which shows that when  $\Gamma_w \rightarrow 0$  and  $\Gamma_w \rightarrow +\infty$ , the efficiency on both cases are zero. Known the fact that efficiency is always a positive number, we can assert that the only extremum we found is a global maximum. With the optimal load, we can get the maximized steady state efficiency  $\eta_{s,max}$

$$\eta_{s,max} = \frac{\frac{\kappa^2}{\Gamma_{re}\Gamma_{tr}}}{(1 + \sqrt{1 + \frac{\kappa^2}{\Gamma_{re}\Gamma_{tr}}})^2}. \quad (2.22)$$

(2.22) shows that  $\frac{\kappa^2}{\Gamma_{tr}\Gamma_{re}}$  is a key term to determine the optimal efficiency, hence it is known as the figure of merit of this system. When the figure of merit is much greater than 1, the system can get high efficiency. From this example, we can see that CMT is a handy tool to analyze a magnetic resonant coupling WPT system, and Karalis et al showed that this analysis is quite accurate in their work [9].



## 2.2 BRIEF REVIEW OF EQUIVALENT CIRCUIT METHOD

Equivalent circuit method is a commonly used method to analyze the behavior of a resonator and coupling between resonators, where resonators are treated as equivalent RLC circuits and the coupling depends on the mutual inductance between inductors. In this section, a two-resonator witrlicity system will be analyzed using the equivalent circuit method to show how the equivalent method works.

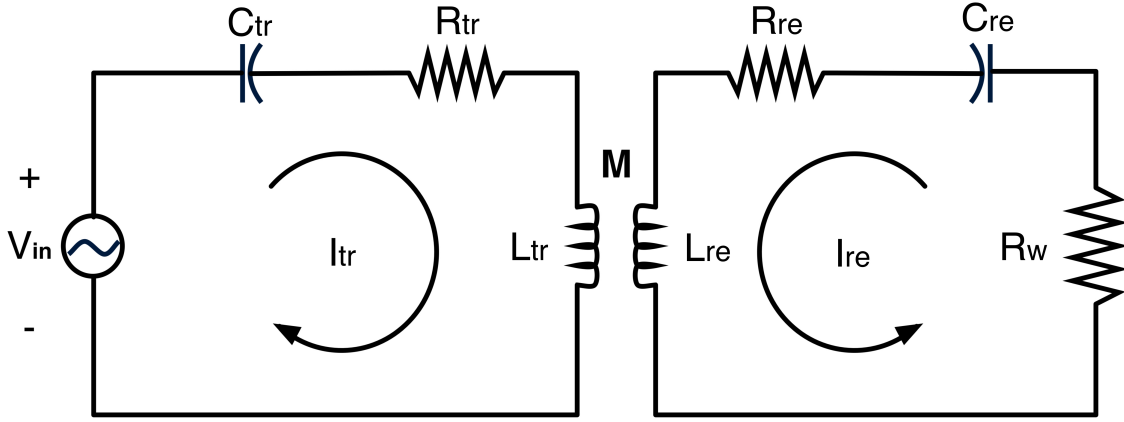


Figure 11: Equivalent circuit of a two-resonator magnetic resonant coupling WPT system

The equivalent circuit of a two-resonator magnetic resonant coupling WPT system is shown in Figure 11 and using KVL, we get the following equations:

$$\begin{bmatrix} R_{tr} + jX_{tr} & j\omega M \\ j\omega M & R_{re} + R_w + jX_{re} \end{bmatrix} \begin{bmatrix} I_{tr} \\ I_{re} \end{bmatrix} = \begin{bmatrix} V_{in} \\ 0 \end{bmatrix}. \quad (2.23)$$

$I_{tr}$  and  $I_{re}$  can be solved and the result is:

$$\begin{aligned} I_{tr} &= \frac{(R_{re} + R_w + jX_{re})V_{in}}{R_{tr}(R_{re} + R_w) - X_{tr}X_{re} + \omega^2 M^2 + j[R_{tr}X_{re} + (R_{re} + R_w)X_{tr}]} \\ I_{re} &= \frac{-j\omega MV_{in}}{R_{tr}(R_{re} + R_w) - X_{tr}X_{re} + \omega^2 M^2 + j[R_{tr}X_{re} + (R_{re} + R_w)X_{tr}]} \end{aligned} \quad (2.24)$$

The efficiency can be expressed as

$$\eta = \frac{|I_{re}|^2 R_w}{\Re\{V_{in} I_{tr}^*\}}. \quad (2.25)$$

Plugging (2.24) into (2.25), we get

$$\eta = \frac{\omega^2 M^2 R_w}{R_{tr}(R_{re} + R_w)^2 + (R_{re} + R_w)\omega^2 M^2 + X_{re}^2 R_{tr}}. \quad (2.26)$$

Define the denominator as  $D(X_{tr}, X_{re})$ , and we can minimize D to maximize the efficiency. Clearly, D is maximized when  $X_{re} = 0$ , which means the system is driven at the resonant frequency of the receiving resonator, and the efficiency becomes

$$\eta|_{X_{re}=0} = \frac{\omega^2 M^2 R_w}{R_{tr}(R_{re} + R_w)^2 + (R_{re} + R_w)\omega^2 M^2}. \quad (2.27)$$

To find the optimal Load, we set  $\partial\eta|_{X_{re}=0}/\partial R_w = 0$  and solve for the load

$$R_{w,opt} = \sqrt{\frac{R_{re}}{R_{tr}}\omega^2 M^2 + R_{re}^2}. \quad (2.28)$$

To make sure that the obtained load is optimal, usually we need to verify that the second derivative is positive. However, here by inspecting (2.27), we find the efficiency is always positive and goes to 0 when  $R_w$  goes to 0 or  $+\infty$ , so the only extremum we found have to be a maximum point. Hence the optimal efficiency is

$$\eta_{opt} = \frac{\frac{\omega^2 M^2}{R_{tr}R_{re}} \sqrt{\frac{\omega^2 M^2}{R_{tr}R_{re}} + 1}}{(2 + \frac{\omega^2 M^2}{R_{tr}R_{re}})(1 + \sqrt{\frac{\omega^2 M^2}{R_{tr}R_{re}} + 1})}. \quad (2.29)$$

Calculating  $\partial\eta_{opt}/\partial\frac{\omega^2 M^2}{R_{tr}R_{re}}$ , we found that it is always greater than 0, so a greater value of  $\frac{\omega^2 M^2}{R_{tr}R_{re}}$  gives us larger efficiency. This conclusion is quite similar as the result we get using CMT.

### 2.3 COMPARING CMT AND EQC METHODS

To compare CMT and equivalent circuit method, The results of analyzing a two-resonator WPT system using CMT and EQC methods are listed below.

$$\begin{aligned}
\Gamma_{w,opt,CMT} &= \sqrt{\Gamma_{re}^2 + \kappa^2 \frac{\Gamma_{re}}{\Gamma_{tr}}} \\
\eta_{max,CMT} &= \frac{\frac{\kappa^2}{\Gamma_{re}\Gamma_{tr}}}{(1 + \sqrt{1 + \frac{\kappa^2}{\Gamma_{re}\Gamma_{tr}}})^2} \\
R_{w,opt,EQC} &= \sqrt{\frac{R_{re}}{R_{tr}} \omega^2 M^2 + R_{re}^2} \\
\eta_{max,EQC} &= \frac{\frac{\omega^2 M^2}{R_{tr}R_{re}} \sqrt{\frac{\omega^2 M^2}{R_{tr}R_{re}} + 1}}{(2 + \frac{\omega^2 M^2}{R_{tr}R_{re}})(1 + \sqrt{\frac{\omega^2 M^2}{R_{tr}R_{re}} + 1})} \\
&= \frac{\frac{\omega^2 M^2}{R_{tr}R_{re}}}{(\frac{1}{\sqrt{\frac{\omega^2 M^2}{R_{tr}R_{re}} + 1}} + \sqrt{\frac{\omega^2 M^2}{R_{tr}R_{re}} + 1})(1 + \sqrt{\frac{\omega^2 M^2}{R_{tr}R_{re}} + 1})}. \tag{2.30}
\end{aligned}$$

(2.30) shows that CMT and EQC give similar results, especially for the optimal load.  $\Gamma_{w,opt,CMT}$  and  $R_{w,opt,EQC}$  are in quite similar form, because  $\Gamma_{re}$  and  $\Gamma_{tr}$  are the intrinsic losses of two resonators, which are physically correlated to the resistances of the resonator,  $R_{tr}$  and  $R_{re}$ , also both  $\omega M$  and  $\kappa$  indicate the coupling between the two resonators. The form of  $\eta_{max,CMT}$  is different from that of  $\eta_{max,EQC}$ , however, when  $\frac{\omega^2 M^2}{R_{tr}R_{re}} \gg 1$ , which is usually satisfied in applications, they give similar results.

Both CMT and EQC are linear approximations of the real system, but they have different pros and cons. CMT is mathematically elegant. The whole system can be described as a set of linear differential equations and the model can be easily expanded to multiple resonators by adding more equations. A major disadvantage of CMT is that the parameters don't have clear physical meaning, so it is difficult to set these parameters to certain values and we can only measure these parameters indirectly. For EQC, the physical meaning is clear but it is difficult to expand the system. As the author will discuss the multiple-resonator system, the CMT method is used in this thesis.

### 3.0 METHODS

#### 3.1 THEORETICAL ANALYSIS

As the efficiency decreases when the distance between the transmitting and the receiving resonators increases, it would be helpful to consider the effect of a relay resonator put between the transmitting and receiving resonators as shown in Figure 12.

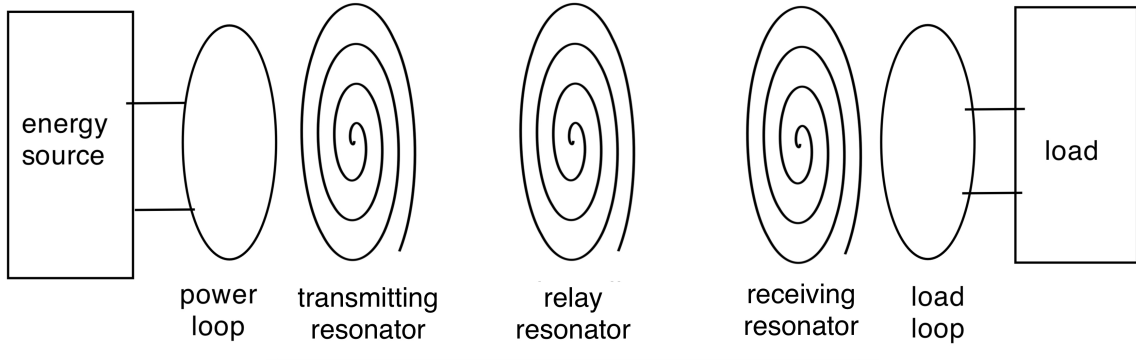


Figure 12: Witricity system with relay.

The CMT equations for multiple-resonator system are

$$\dot{a}_m(t) = (j\omega_0 - \Gamma_m - \Gamma_{mw})a_m(t) + j \sum_{n=0, n \neq m}^{N-1} \kappa_{mn}a_n(t) + f_m(t) \quad (3.1)$$

where  $N$  is the total number of resonators,  $\Gamma_m$  and  $\Gamma_{mw}$  are the intrinsic loss and the load of the  $m^{th}$  resonator respectively,  $\kappa_{mn}$  is the coupling coefficient between the  $m^{th}$  and  $n^{th}$  resonators and  $f_m$  is the input into the  $m^{th}$  resonator.

In the relay case, we consider only three resonators, namely transmitting, relay and receiving resonators. Only the transmitting resonator is powered by an external source and only the receiving resonator has a load. To further simplify the problem, we ignore the coupling between transmitting and receiving resonators because they are separated by a longer distance. So, the differential equations for this case becomes

$$\begin{aligned}\dot{a}_{tr}(t) &= (j\omega_0 - \Gamma_{tr})a_{tr}(t) + j\kappa_{trr}a_r(t) + f(t) \\ \dot{a}_r(t) &= (j\omega_0 - \Gamma_r)a_r(t) + j\kappa_{trr}a_{tr}(t) + j\kappa_{rre}a_{re}(t) \\ \dot{a}_{re}(t) &= (j\omega_0 - \Gamma_{re} - \Gamma_w)a_{re}(t) + j\kappa_{rre}a_r(t).\end{aligned}\tag{3.2}$$

where tr, r and re are short for transmitting, relay and receiving. Assuming that the system is driven by a source with the frequency equal to the natural frequency  $\omega_0$ , at steady state,  $a_{tr}$ ,  $a_r$  and  $a_{re}$  all have the time dependent term  $e^{j\omega_0 t}$ , so in steady state, (3.2) becomes

$$\begin{aligned}\Gamma_{tr}a_{trs} &= j\kappa_{trr}a_{rs} + f \\ \Gamma_r a_{rs} &= j\kappa_{trr}a_{trs} + j\kappa_{rre}a_{res} \\ (\Gamma_{re} + \Gamma_w)a_{res} &= j\kappa_{rre}a_{rs}.\end{aligned}\tag{3.3}$$

where  $a_{trs}$ ,  $a_{rs}$  and  $a_{res}$  are the positive frequency components in steady state. Write the last two equations into matrix form, and we have

$$\begin{bmatrix} \Gamma_r & -j\kappa_{rre} \\ -j\kappa_{rre} & \Gamma_{re} + \Gamma_w \end{bmatrix} \begin{bmatrix} a_r/a_{tr} \\ a_{re}/a_{tr} \end{bmatrix} = \begin{bmatrix} j\kappa_{trr} \\ 0 \end{bmatrix}.\tag{3.4}$$

This way we can solve for  $a_r/a_{tr}$  and  $a_{re}/a_{tr}$

$$\begin{bmatrix} a_r/a_{tr} \\ a_{re}/a_{tr} \end{bmatrix} = \frac{1}{\Gamma_r(\Gamma_{re} + \Gamma_w) + \kappa_{rre}^2} \begin{bmatrix} j\kappa_{trr}(\Gamma_{re} + \Gamma_w) \\ -\kappa_{rre}\kappa_{trr} \end{bmatrix}.\tag{3.5}$$

Now we can start to analyze the steady state efficiency. From CMT, the efficiency can be expressed as

$$\eta_s = \frac{2\Gamma_w|a_{res}|^2}{2\Gamma_{tr}|a_{trs}|^2 + 2\Gamma_r|a_{rs}|^2 + 2(\Gamma_{re} + \Gamma_w)|a_{res}|^2}.\tag{3.6}$$

Here the numerator is the power used to drive the load and the denominator is the total power consumption of the system, which, in steady state, is the same as power going into the system. Dividing both the numerator and denominator by  $|a_{trs}|^2$ , we get

$$\eta_s = \frac{2\Gamma_w \left| \frac{a_{res}}{a_{trs}} \right|^2}{2\Gamma_{tr} + 2\Gamma_r \left| \frac{a_{rs}}{a_{trs}} \right|^2 + 2(\Gamma_{re} + \Gamma_w) \left| \frac{a_{res}}{a_{trs}} \right|^2}. \quad (3.7)$$

Plug in (3.5), and the efficiency becomes

$$\eta_s = \frac{\Gamma_w \kappa_{rre}^2 \kappa_{trr}^2}{\Gamma_{tr} [\Gamma_r (\Gamma_{re} + \Gamma_w) + \kappa_{rre}^2]^2 + \Gamma_r \kappa_{trr}^2 (\Gamma_{re} + \Gamma_w)^2 + (\Gamma_{re} + \Gamma_w) \kappa_{rre}^2 \kappa_{trr}^2}. \quad (3.8)$$

Setting  $\partial\eta_s/\partial\kappa_{rre} = 0$ , we have

$$\kappa_{rre} = \sqrt[4]{(\Gamma_{re} + \Gamma_w)^2 (\Gamma_r^2 + \frac{\Gamma_r}{\Gamma_{tr}} \kappa_{trr}^2)}. \quad (3.9)$$

The obtained  $\kappa_{rre}$  was verified to be a maximum point by calculating the second derivative. (3.9) shows that the optimal relay position is affected by the load value, because the coupling coefficient is negatively correlated with distance between resonators. More precisely, when we increase the load value, we should move the relay resonator toward the device resonator to get maximum efficiency.

Plug (3.9) back into (3.8), and the result is

$$\eta_s = \frac{\Gamma_w \kappa_{trr}^2 \sqrt{\Gamma_r^2 + \frac{\Gamma_r}{\Gamma_{tr}} \kappa_{trr}^2}}{(\Gamma_{re} + \Gamma_w) [\Gamma_{tr} (\Gamma_r + \sqrt{\Gamma_r^2 + \frac{\Gamma_r}{\Gamma_{tr}} \kappa_{trr}^2})^2 + \kappa_{trr}^2 (\Gamma_r + \sqrt{\Gamma_r^2 + \frac{\Gamma_r}{\Gamma_{tr}} \kappa_{trr}^2})]}. \quad (3.10)$$

$\eta_s$  is now a function of  $\Gamma_w$ , so the next task is to find the optimal load to maximize the steady state efficiency. To do this, we calculate  $\partial\eta_s/\partial\Gamma_w$  from (3.10), and the result shows

that  $\partial\eta_s/\partial\Gamma_w$  is always positive, which means that larger load will give us higher efficiency. Actually we can see from (3.10) that when  $\Gamma_w \gg \Gamma_d$ ,  $\eta_s$  tends to a constant.

$$\begin{aligned}
\eta_{s,\Gamma_w \gg \Gamma_{re}} &= \frac{\kappa_{trr}^2 \sqrt{\Gamma_r^2 + \frac{\Gamma_r}{\Gamma_{tr}} \kappa_{trr}^2}}{\Gamma_{tr}(\Gamma_r + \sqrt{\Gamma_r^2 + \frac{\Gamma_r}{\Gamma_{tr}} \kappa_{trr}^2})^2 + \kappa_{trr}^2(\Gamma_r + \sqrt{\Gamma_r^2 + \frac{\Gamma_r}{\Gamma_{tr}} \kappa_{trr}^2})} \\
&= \frac{\frac{\kappa_{trr}^2}{\Gamma_{tr}\Gamma_r} \sqrt{1 + \frac{\kappa_{trr}^2}{\Gamma_{tr}\Gamma_r}}}{(1 + \sqrt{1 + \frac{\kappa_{trr}^2}{\Gamma_{tr}\Gamma_r}})^2 + \frac{\kappa_{trr}^2}{\Gamma_{tr}\Gamma_r}(1 + \sqrt{1 + \frac{\kappa_{trr}^2}{\Gamma_{tr}\Gamma_r}})} \\
&= \frac{1 + \frac{\kappa_{trr}^2}{\Gamma_{tr}\Gamma_r} - \sqrt{1 + \frac{\kappa_{trr}^2}{\Gamma_{tr}\Gamma_r}}}{1 + \frac{\kappa_{trr}^2}{\Gamma_{tr}\Gamma_r} + \sqrt{1 + \frac{\kappa_{trr}^2}{\Gamma_{tr}\Gamma_r}}} \\
&= 1 - \frac{2}{1 + \sqrt{1 + \frac{\kappa_{trr}^2}{\Gamma_{tr}\Gamma_r}}}. \tag{3.11}
\end{aligned}$$

(3.11) shows that  $\frac{\kappa_{trr}^2}{\Gamma_{tr}\Gamma_r}$  is an important parameter to determine the maximum efficiency of the system and the larger this parameter is the higher efficiency we can get.

## 3.2 EXPERIMENTS

### 3.2.1 RESONATOR DESIGN

resonators are the most important component in a magnetic resonant coupling system, and one of the most important features of a good resonator is that it must have a high Q factor. Solenoid is known to have the highest Q factor among all the resonator structures, however, due to its 3D structure solenoid is not convenient in use, especially for implanted devices, where the volume of resonator have to be as small as possible. So in our experiment, spiral coils were used, which can be printed easily on a board, and the resonant frequency can be adjusted by attaching metal pieces on the back of coils.

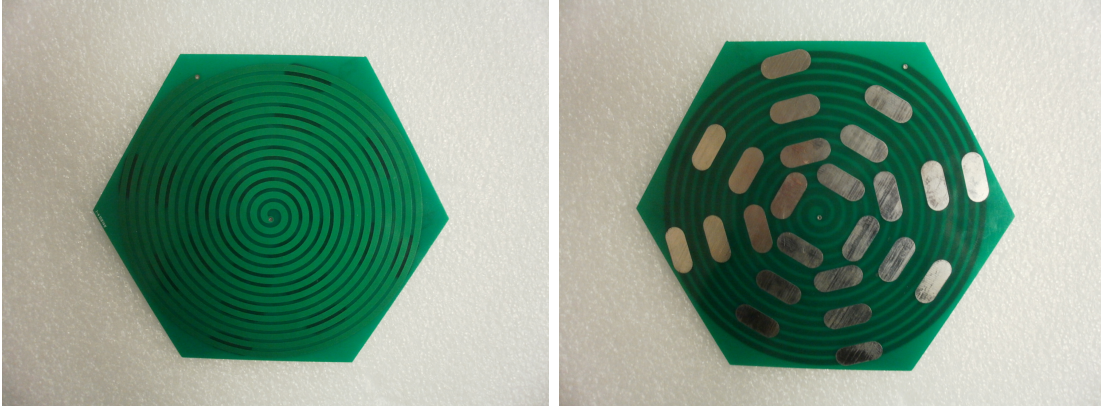


Figure 13: Self-resonant coil used in the experiment.

Figure 13 shows the resonator used in the experiment. It is a regularly hexagonal PCB with a printed spiral coil, 2.6 inch in diameter, 0.11 inch in trace width with a 0.06-inch trace spacing.

### 3.2.2 PARAMETER MEASUREMENT

There are three parameters need to be measured, namely Q factor, resonant frequency and coupling coefficient. However, before we get into this topic, another issue needs to be considered. For such a high frequency, clipper is no longer a good idea to connect the source and the coil, while a source loop shows better performance, which can couple with the coil through magnetic induction.

#### 3.2.2.1 SOURCE LOOP MANUFACTURING

In our experiment, we made a source loop using the same idea as a magnetic field probe [28]. A  $50\Omega$  coaxial cable was used to make the loop, so that the match between source and the loop will not be an issue. The cable was winded into a circle and both the shield and the inner metal at the end are connect to the shield and a small gap was opened on the shield at the top as shown in Figure 14. The diameter of the loop we made is approximately the same as the outer diameter of our spiral to make sure the two of them can couple well.



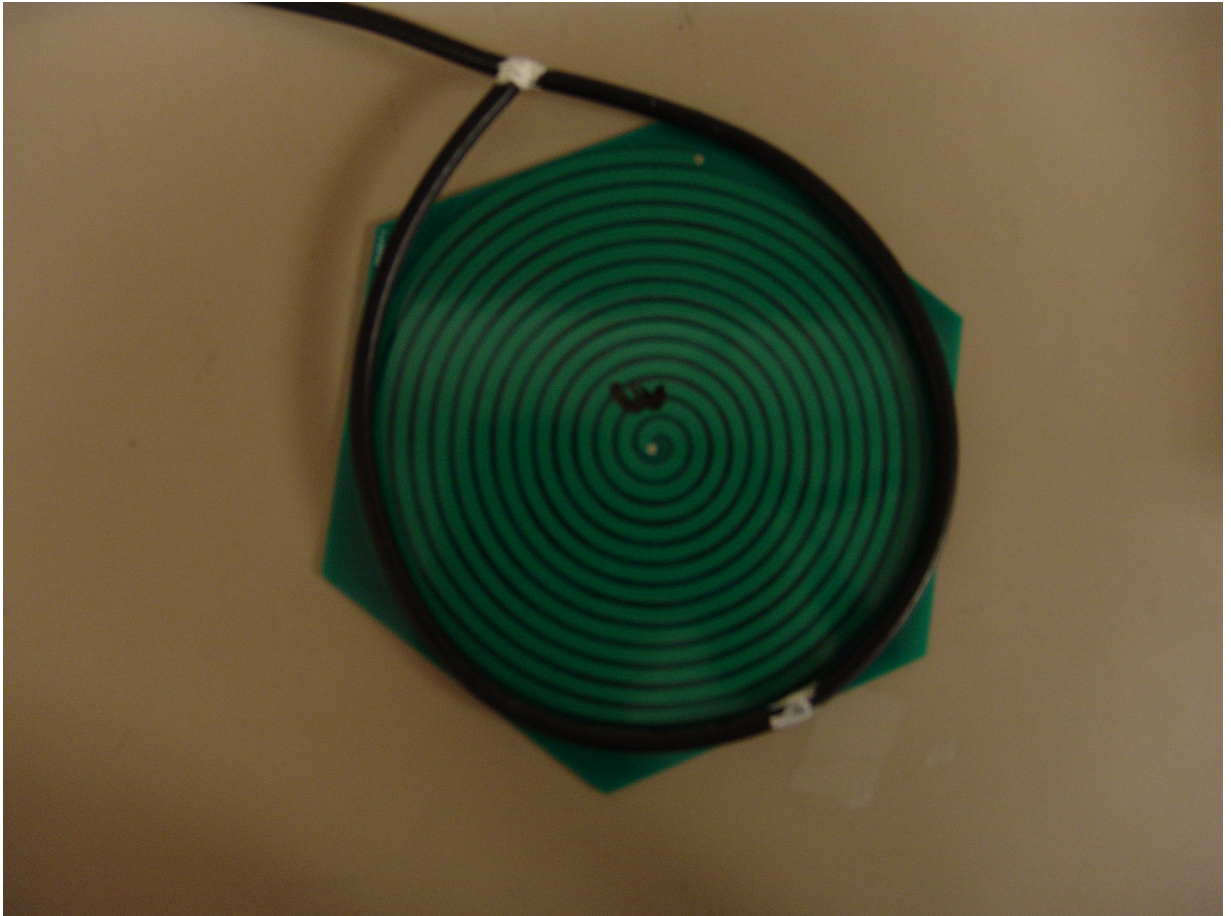


Figure 14: Source loop.

### 3.2.2.2 NATURAL FREQUENCY, Q FACTOR AND COUPLING COEFFICIENT MEASUREMENT

Vector Network Analyzer (VNA) is a common device to measure the parameters of high frequency devices and are used a lot in the research of microwave and RF devices. VNA 2180 from Array Solutions was used in this thesis. Perform a frequency sweep on the coil, and we can get the resonant frequency and Q factor.

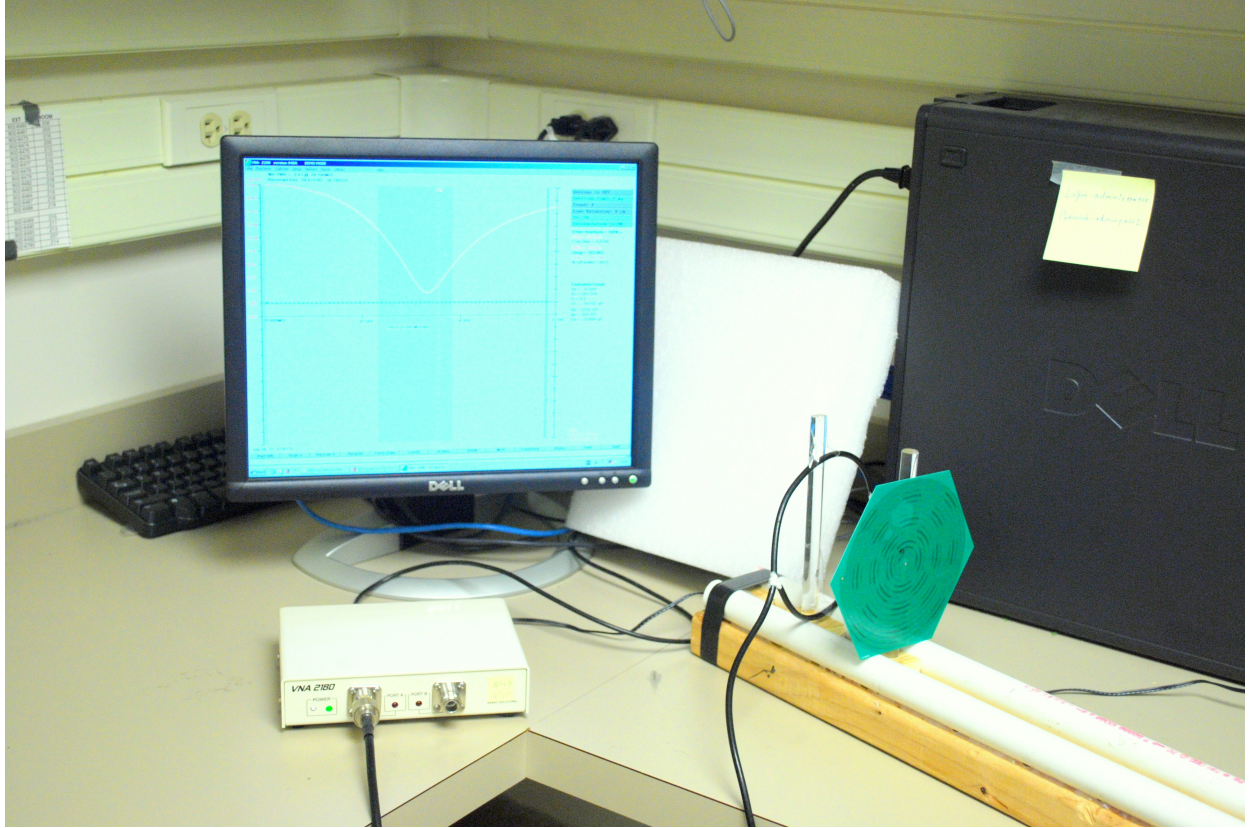


Figure 15: Experimental setup to measure Q factor.

Figure 16 shows the  $S_{11}$  curve in smith chart. From the resonant circle, we can get the resonant frequency  $f_0$  and the bandwidth  $\Delta f$  using the 45-degree method [ref], and the Q factor is  $\frac{f_0}{|f_1-f_2|}$ . The 45-degree method is shown in Figure 16.

One problem is that the  $50\ \Omega$  inner resistance of the VNA becomes a load of the coil through coupling, so the coupling must be weak to get the unloaded Q factor. However,

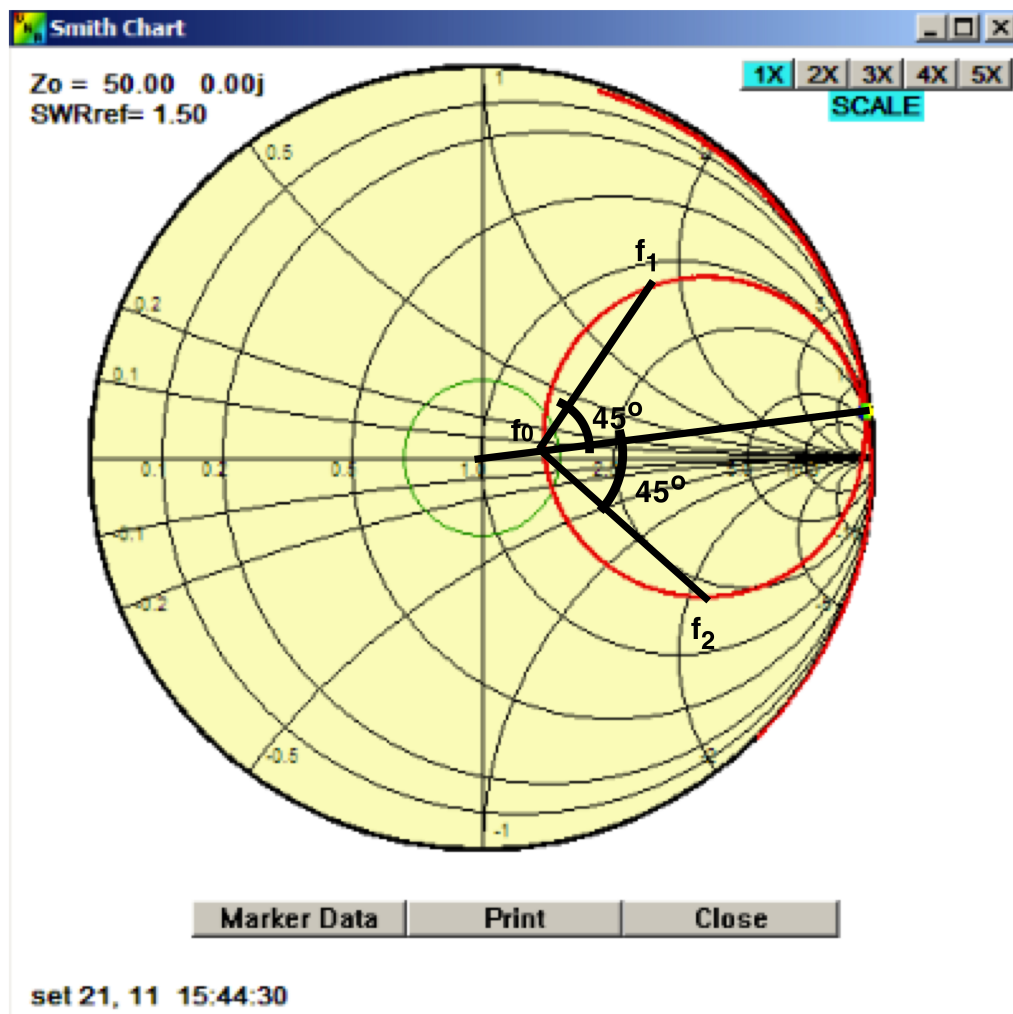


Figure 16:  $S_{11}$  curve in smith chart and 45-degree method to measure Q factor.



when the coupling is too weak, the resonant circle is so small that we can not get an accurate measurement through 45-degree method. Thus, we need to handle this trade-off and find the proper coupling. Some researches show that the effect of the  $50\ \Omega$  inner resistance can be eliminated by (3.12) [29]

$$Q_0 = (1 + \frac{1}{\frac{2}{d} - 1})Q_M \quad (3.12)$$

where  $Q_0$  is the actual unloaded Q factor,  $Q_M$  the measured Q factor and  $d$  the diameter of the resonant circle normalized by radius of the smith chart. Using this adjustment, we can use relatively stronger coupling while still get accurate Q factor.

Measuring the coupling coefficient is a more complicated problem. According to the CMT, coupling coefficient can be measured through measuring the frequency splitting of a two-resonator system. Using VNA, we can measure the two peak frequencies on the standing wave ratio (SWR) curve to determine the frequency splitting and hence get the coupling coefficient using (3.13)

$$\kappa = \pi|f_1 - f_2| \quad (3.13)$$

As coupling coefficient is highly correlated with distance between the two resonators, several measurements were performed with respect to different distances.

### 3.2.3 EFFICIENCY MEASUREMENT

In this experiment, efficiency is our major concern, and we will find the relationship between power transfer efficiency and the relative position of the three resonators. So a platform was made such that four poles were placed on a straight trail and can move freely along the trail. resonators can be attached on the poles as shown in Figure 19.

The power supply from port 1 can be calculated as  $P(1 - |S_{11}|^2)$ , where  $P$  is the total power generated by port 1. The  $50\Omega$  internal resistance in port 2 acts as the load of the system, which can be adjusted by changing the distance between receiving resonator and load loop, and the power consumption on the load is  $P|S_{21}|^2$ . So the efficiency can be calculated as

$$\eta = \frac{|S_{21}|^2}{1 - |S_{11}|^2}. \quad (3.14)$$

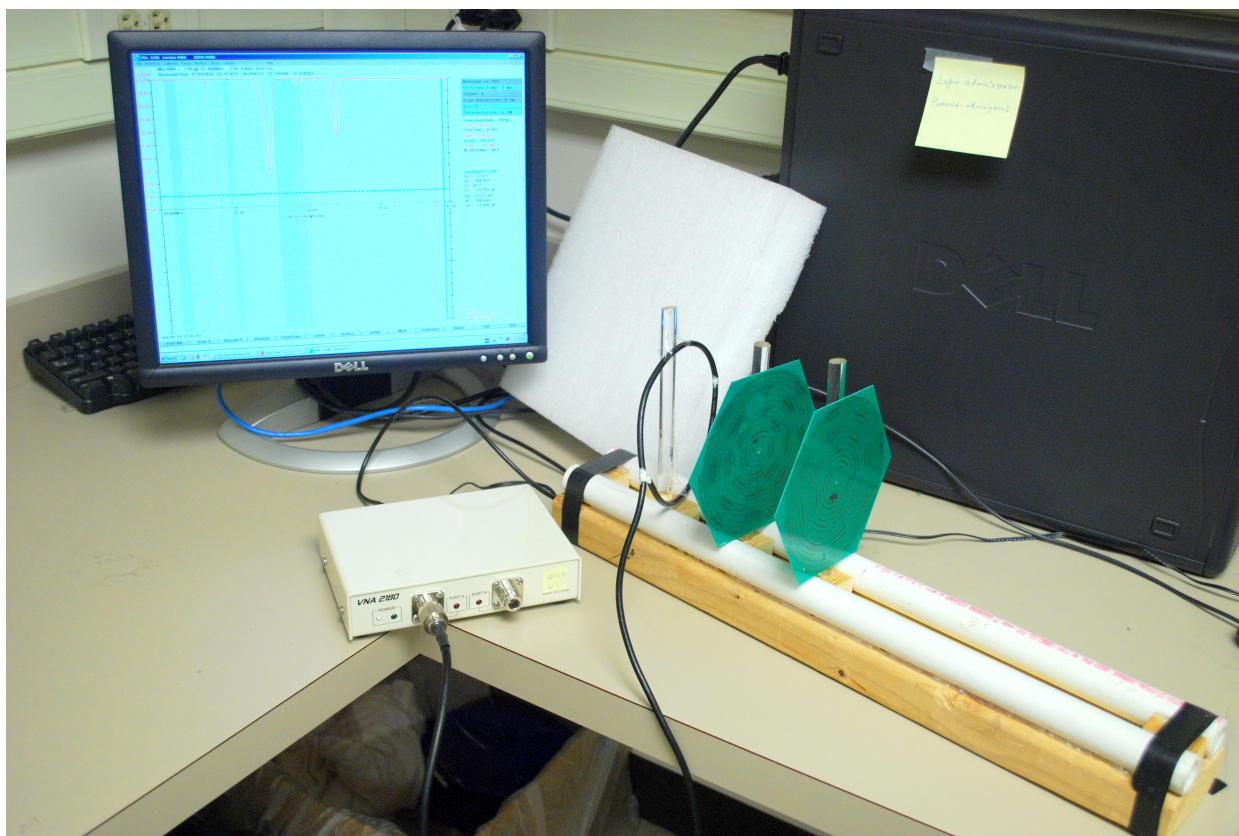


Figure 17: Experimental setup to measure coupling coefficients.

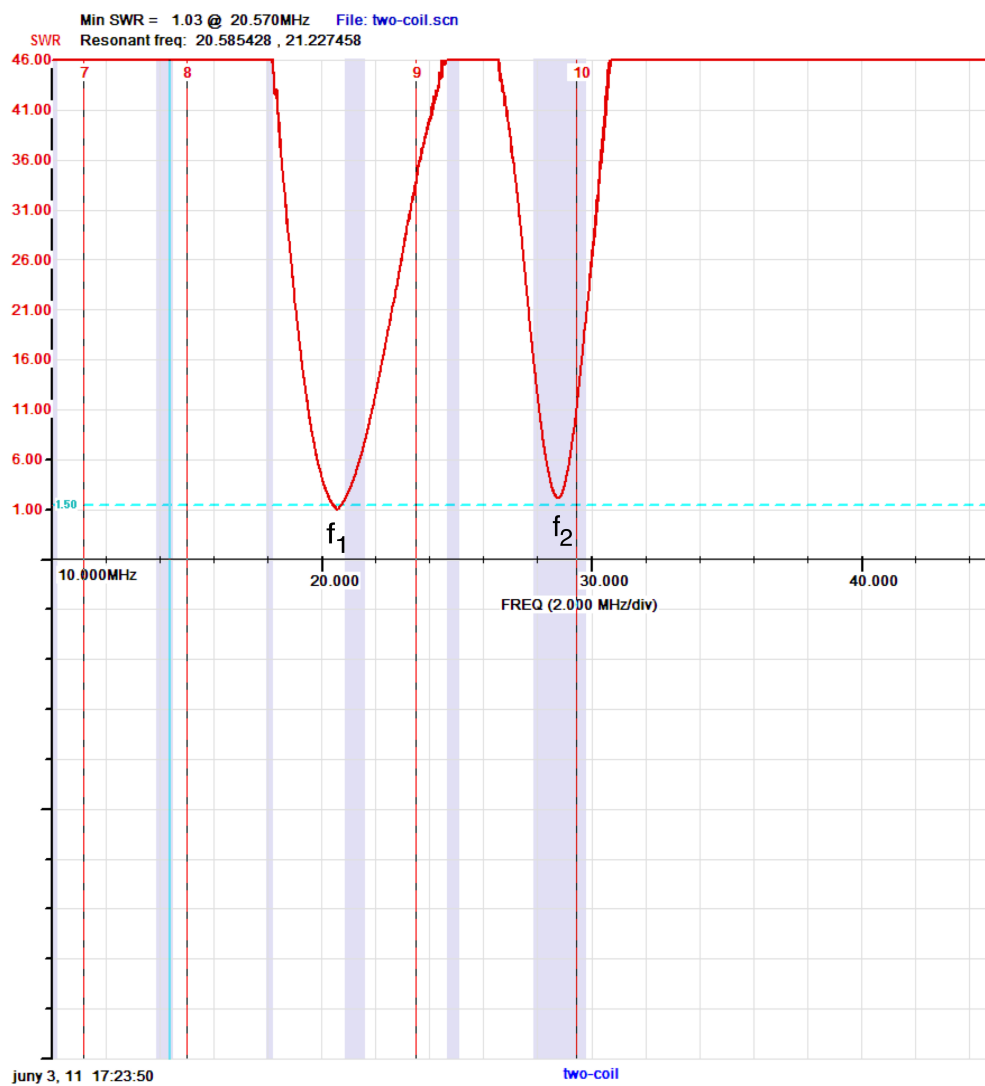


Figure 18: SWR curve of a two-resonator system and frequency splitting method to measure coupling coefficient.

In the experiment, the transmitting resonator and receiving resonator were separated by 7 inches, and efficiency was measured with several different relay positions in between.

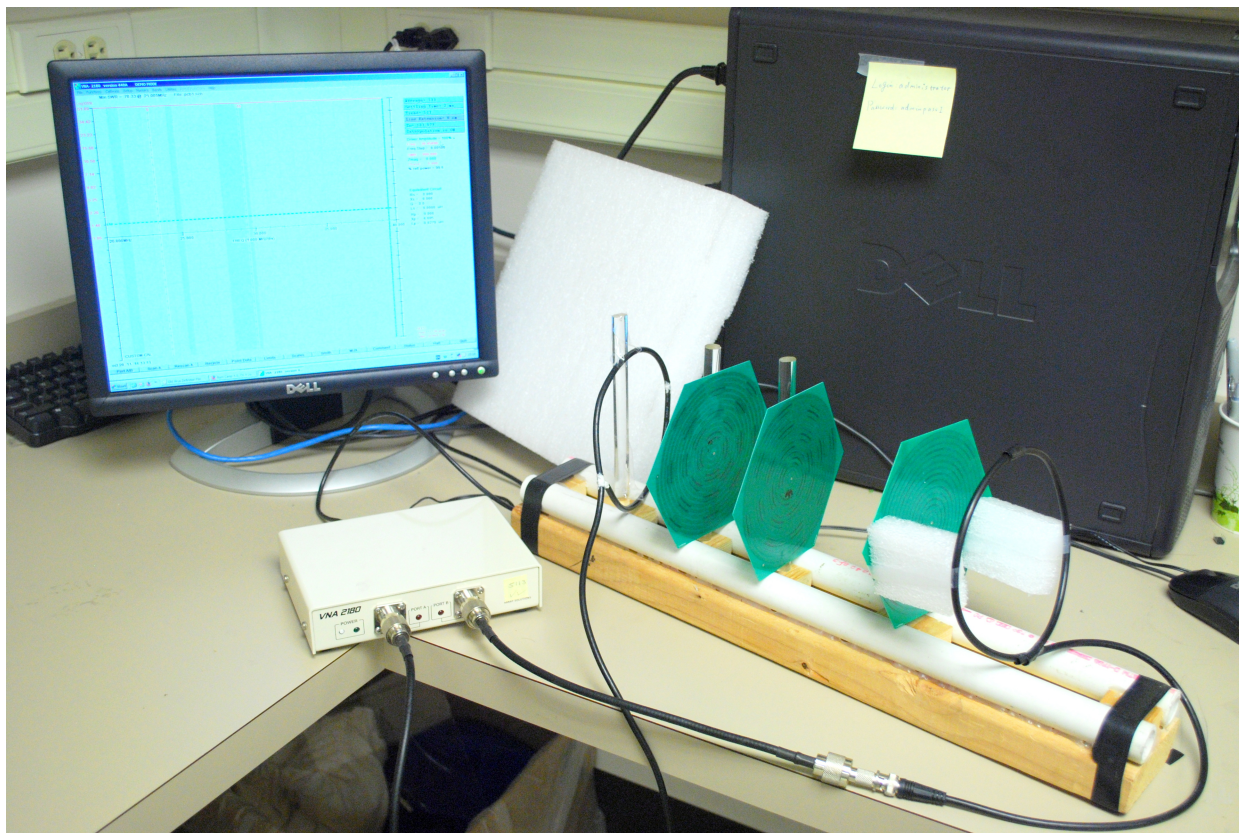


Figure 19: Experimental setup for efficiency measurement

### 3.3 APPLICATIONS

When performing biological experiments on laboratory rodents implanted with miniature devices, a possible problem is that a battery is too heavy for the rodent to carry. In this case, magnetic resonant coupling WPT method is a good solution, where a small receiving resonator is used instead of a battery. However, when the rodent is moving, the transferred power changes, so it is difficult to make sure that sufficient amount of power is transferred



to the implanted devices regardless the locations of rodent in the platform using a simple two-resonator system. To solve this problem, a new platform, including a new multiple-resonator transmitter and a innovative receiving resonator which can be integrated within the container of an implanted device, for performing biological experiments on laboratory rodents was fabricated and tested.

### **3.3.1 MULTIPLE-RESONATOR TRANSMITTER DESIGN**

This transmitter was built up using the hexagonal PCB self-resonant spiral coil introduced before and it will serve as a platform, where rodents run. A seven-resonator transmitter was considered as a simplest case, which is shown in Figure 20. A larger platform can be covered with more resonators. Each resonator in the transmitter was driven by a separated driving loop, so 7 loops were connected in parallel and were located in a pattern shown in Figure 21

### **3.3.2 RECEIVING RESONATOR DESIGN**

Implanted devices are usually protected by a container, and the new receiving resonator was designed so that it can be integrated in the container, which reduced the total volume of implanted devices. The resonator consists three parts. The top and bottom parts are two identical planar spirals which start with an outer diameter of 1 inch and spirals inward with a pitch of 0.008 inch for approximately 30 turns., and the side surface is a solenoid with a 0.25-inch height. The Q factor and resonant frequency were measured to be 61 and 30.14 MHz, respectively.

### **3.3.3 POWER TRANSFER MEASUREMENT**

To evaluate received power with respect to different receiving resonator locations, we measured the induced voltage of several different receiving resonator positions shown in Figure 24. The maximum and minimum induced voltages as well as the standard deviation were evaluated. During experiment, we found that in the aim of getting sufficient power everywhere,



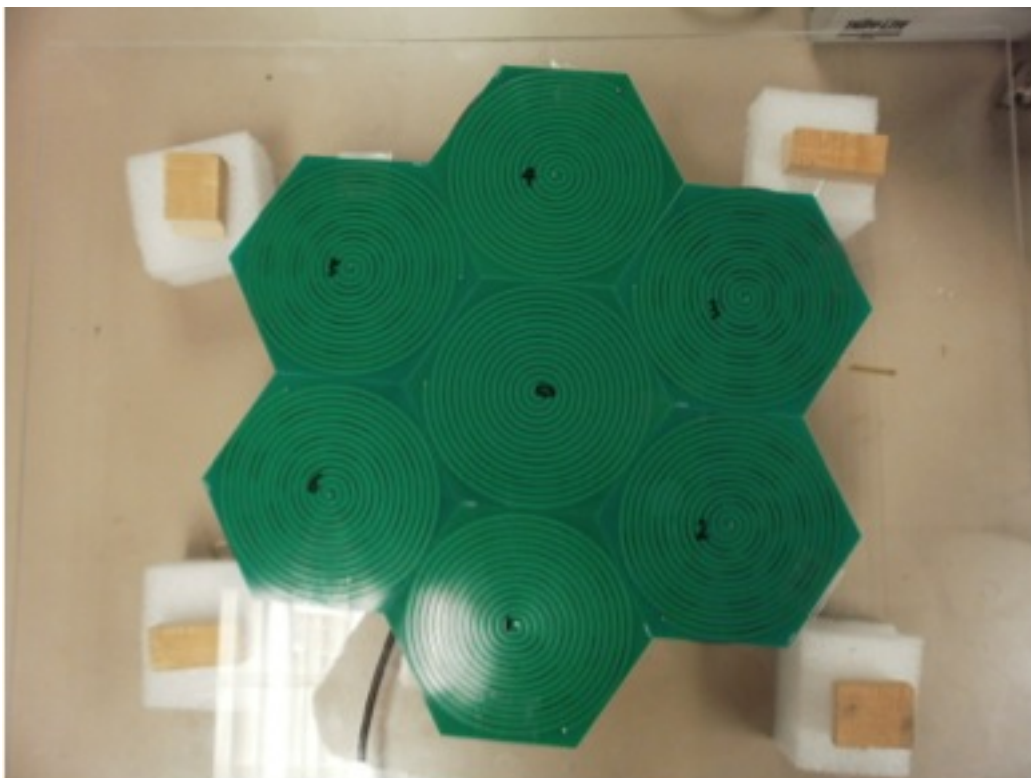


Figure 20: 7-resonator transmitter

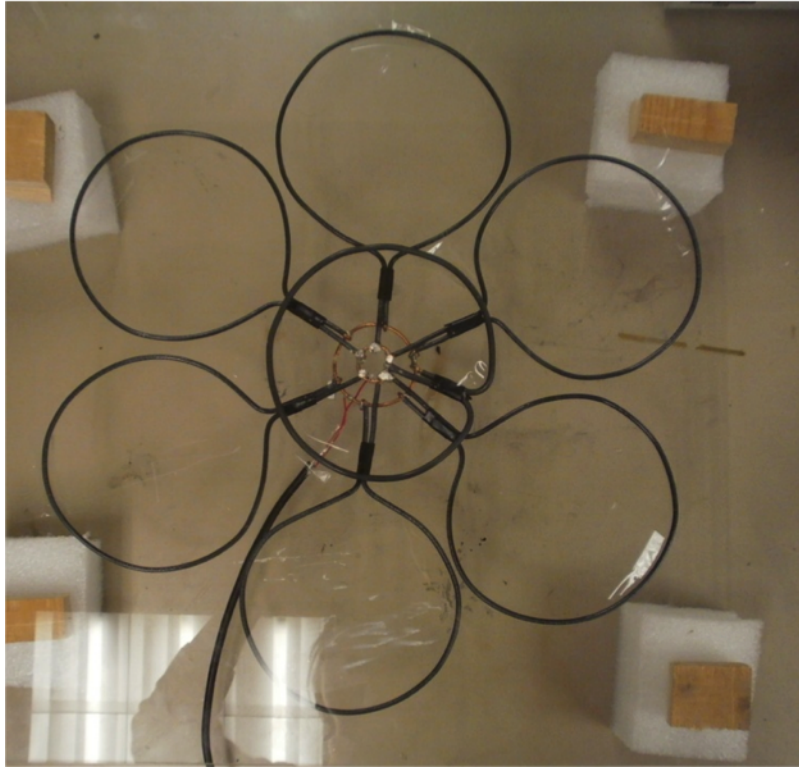


Figure 21: driving loops for multiple-resonator transomitter

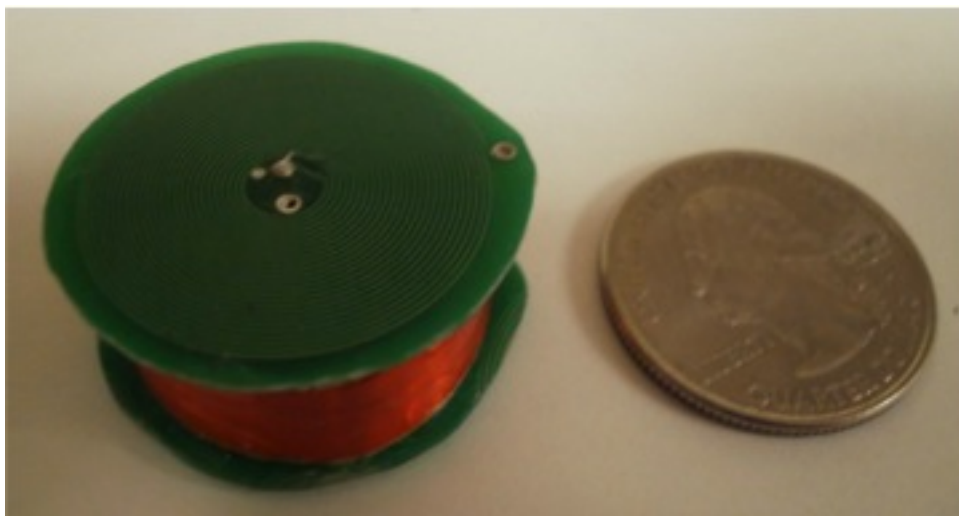


Figure 22: New receiving resonator

the distance between transmitting and receiving resonators is not the smaller the better, so three different distances were measured, and the statistical features were compared.

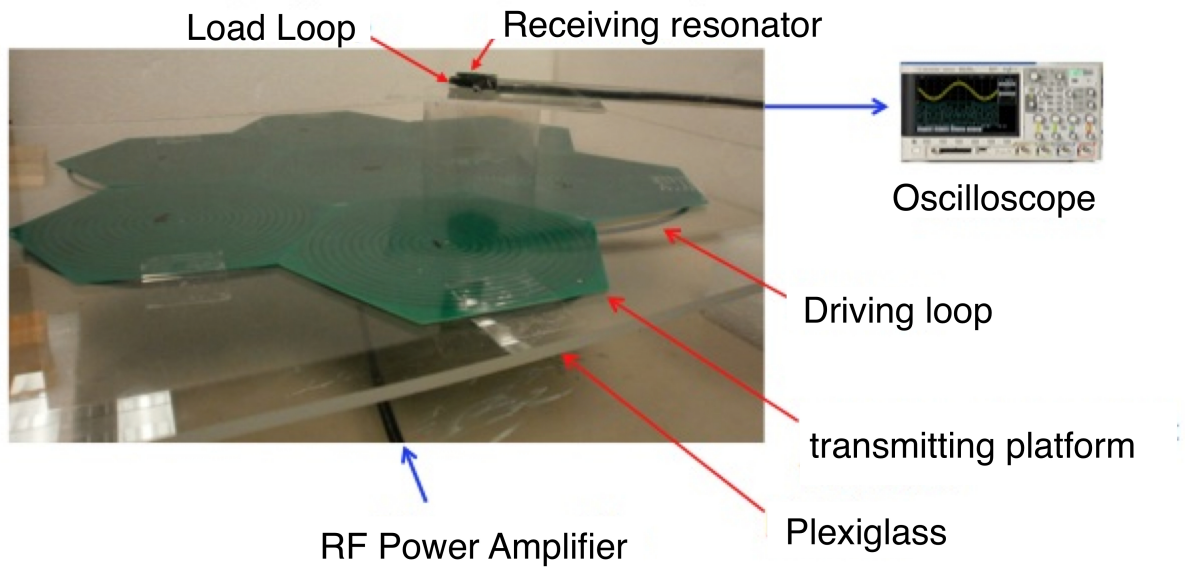


Figure 23: Experimental setup for measuring induced voltage

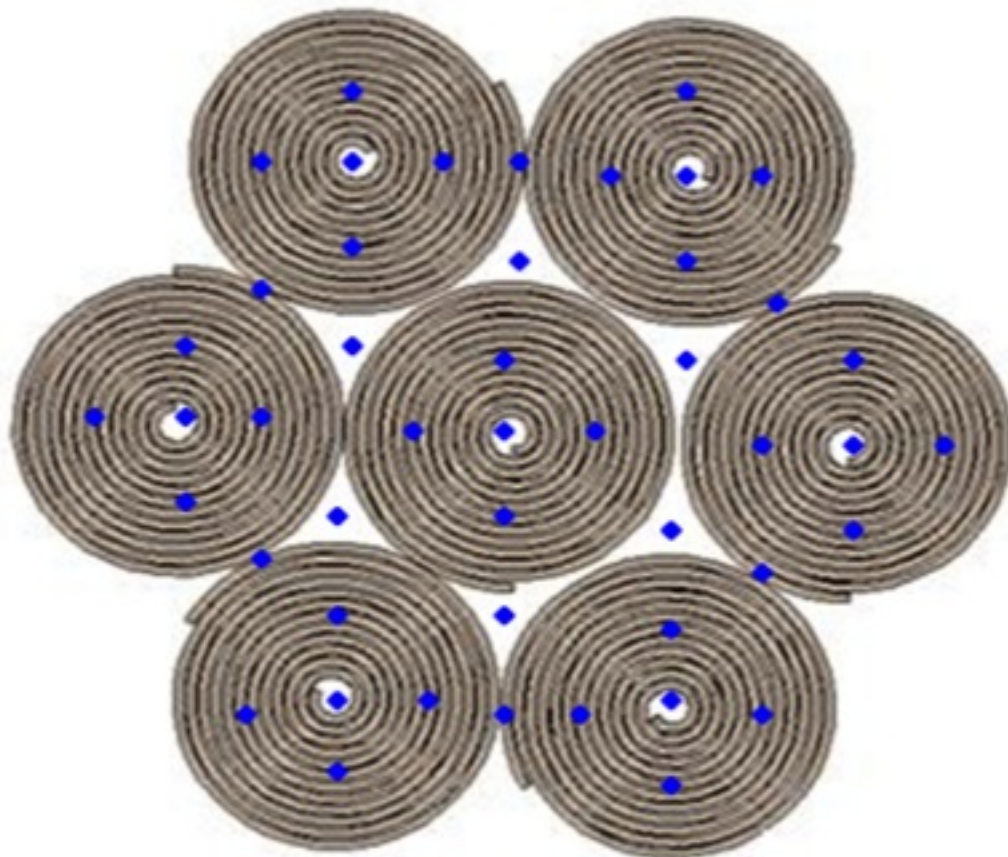


Figure 24: Receiving resonator positions for induced voltage measurement

## 4.0 RESULTS AND DISCUSSIONS

### 4.1 RELAYED WPT SYSTEM

Three coils were used in the experiment, so the intrinsic parameters of each coil were measured, including the resonant frequency and Q factor, and the intrinsic loss can be calculated from Q factor and resonant frequency using (4.1):

$$\Gamma = \frac{\omega_0}{2Q}. \quad (4.1)$$

The result is shown in Table 1.

Table 1: Resonant frequency, Q factor and Intrinsic loss

Coils	Source	Relay	Device
Resonant frequency (MHz)	29.45	29.44	29.49
Q factor	110	107.6	107.9
Intrinsic loss (rad/s)	$1.85 \times 10^5$	$2.64 \times 10^5$	$1.85 \times 10^5$

Then the coupling parameter was measured with different distances between two coils. The curve  $\kappa$  vs. distance is shown in Figure 25, with the distance from 1.25 inches to 7 inches and the step is 0.25 inch.

Figure 25 shows that coupling coefficient decreases at approximately the same speed as  $d^{-2}$ .

To calculate the efficiency, the S parameters  $S_{11}$  and  $S_{21}$  were measured. Firstly the source coil and device coil were fixed on the platform with a 7-inch distance. The efficiency

Table 2:  $\kappa$  vs distance

distance(inch)	$f_1$ (MHz)	$f_2$ (MHz)	$\kappa$ (Mrad/s)
1.25	24.9	36.1	35.35
1.50	25.4	35.3	31.08
1.75	26.04	34.15	25.49
2.00	26.6	33.2	20.77
2.25	27.1	32.5	17.01
2.50	27.5	32.0	14.05
2.75	27.8	31.6	11.93
3.00	28.1	31.2	9.72
3.25	28.3	30.95	8.31
3.50	28.4	30.75	7.39
3.75	28.55	30.6	6.42
4.00	28.7	30.45	5.64
4.25	28.8	30.3	4.65
4.50	28.9	30.2	4.18
4.75	29.0	30.1	3.53
5.00	29.05	30.03	3.08
5.25	29.09	29.97	2.74
5.50	29.14	29.92	2.44
5.75	29.16	29.86	2.19
6.00	29.23	29.84	1.92
6.25	29.28	29.81	1.67
6.50	29.30	29.77	1.47
6.75	29.32	29.53	0.67
7.00	29.34	29.53	0.59

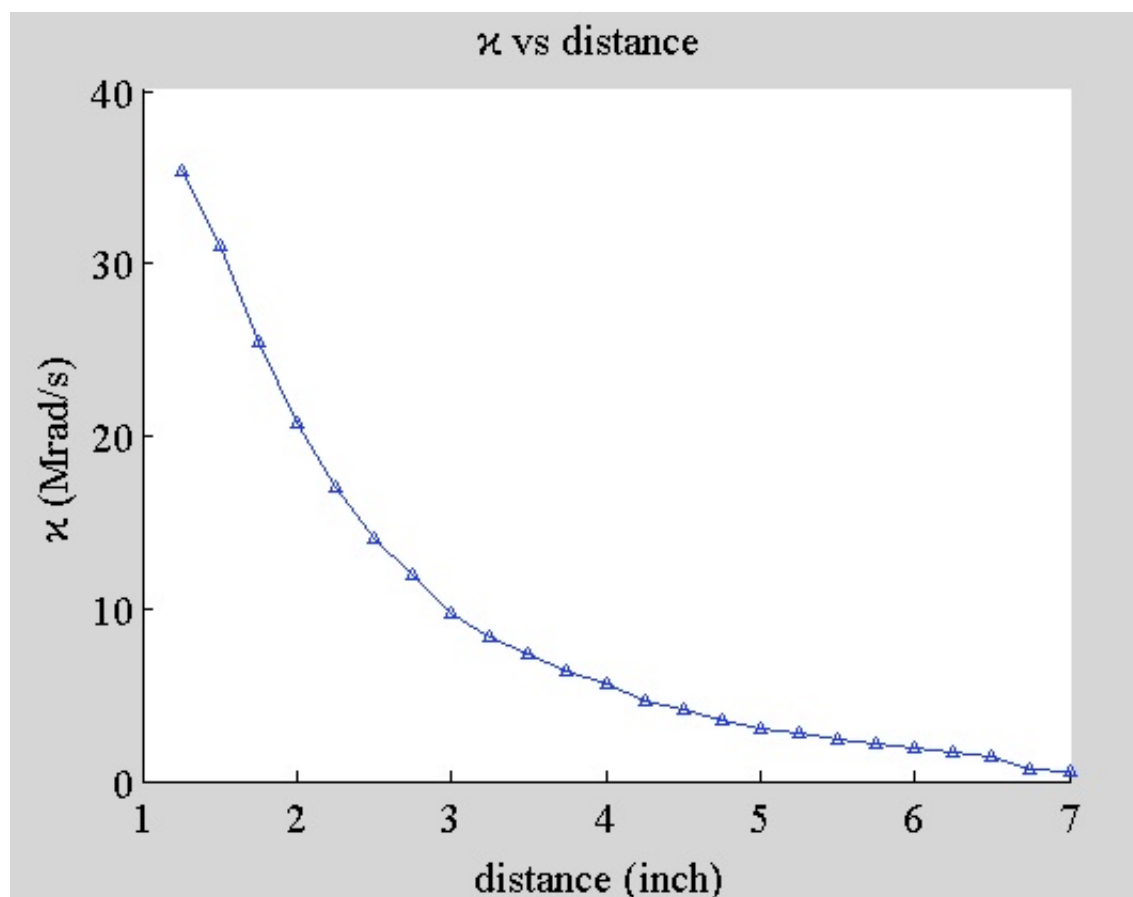


Figure 25:  $\kappa$  vs. distance

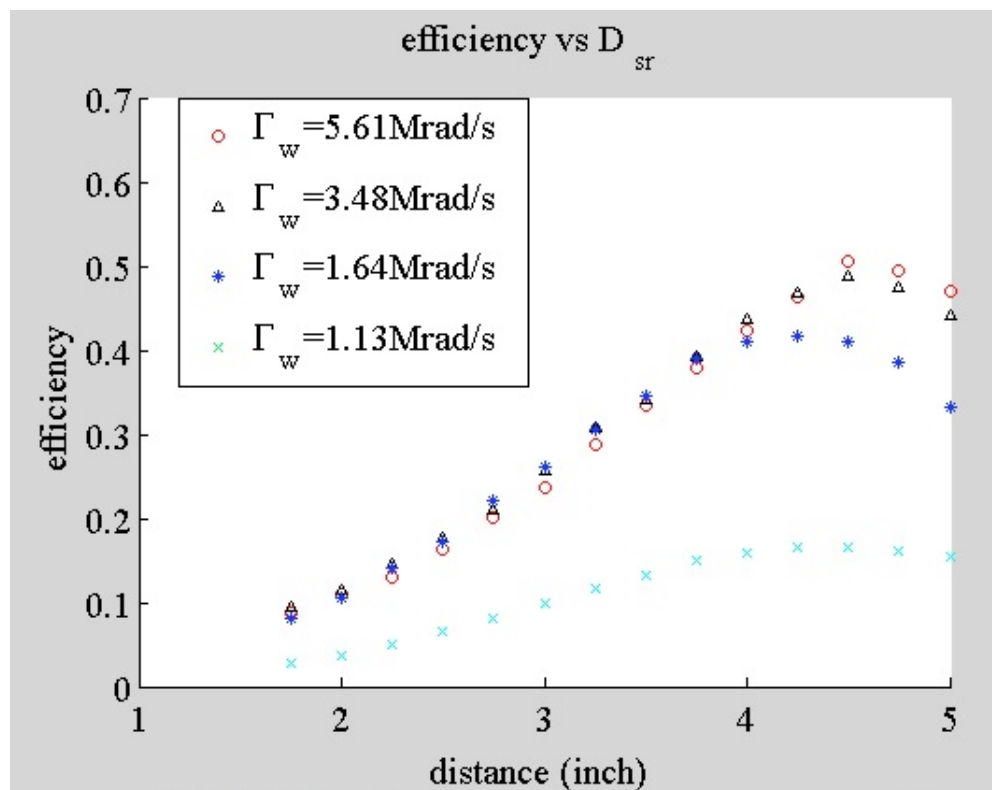


Figure 26: Efficiency vs. distance between S and R.



with no relay is approximately 0, then a relay coil was inserted in between. Efficiency was calculated for different relay position, and in the experiment, the distance between source and relay are set from 2 inches to 5 inches with a 0.25 inch step. The efficiency vs. distance between source and relay coil is shown in Figure 26, which shows that the optimal relay position is correlated with the load value, such that when load value is increased, the optimal relay position moves toward the receiving resonator. Also, this figure shows that by increasing the load value, we can increase the maximum efficiency. The maximum efficiency we measured is above 50%, which is much higher than the case with no relay, this value can be increased by using resonators with higher Q factor, increasing load value and decreasing the energy absorbing objects in the surroundings.

## 4.2 MULTIPLE-COIL-TRANSMITTER POWERING PLATFORM

The induced voltage was measured at the sample points shown in Figure 24 and the distance between transmitting and receiving resonator is set to be 2 inches. Figure 27 shows the measured result, and the statistical analysis result is shown in Table 3. From Table 3 we can see that when distance between transmitting and receiving resonators is 2 inches, the induced voltage showed better uniformness and the minimal induced voltage increased which can make sure the sufficient power transfer even if the devices are at the worst locations. The phenomenon that minimal value increases when distance increases is against our intuition, but a more careful thinking shows that with larger distance, the shift angle between transmitting resonator and receiving resonator is smaller, which means they are more aligned, and this caused the increase of the minimal value. However, in the maximal value case, the receiving resonator is already align with a transmitting resonator, so increasing the distance will not affect the alignment of the two resonators.

Table 3: Statistical features of measured induced voltage

distance(inch)	2	1.65	1.26
Maximal induced Vpp (V)	2.64	3.14	3.80
Minimal induced Vpp (mV)	520	450	340
Mean(V)	1.37	1.56	1.78
Std(V)	1.18	1.44	1.79

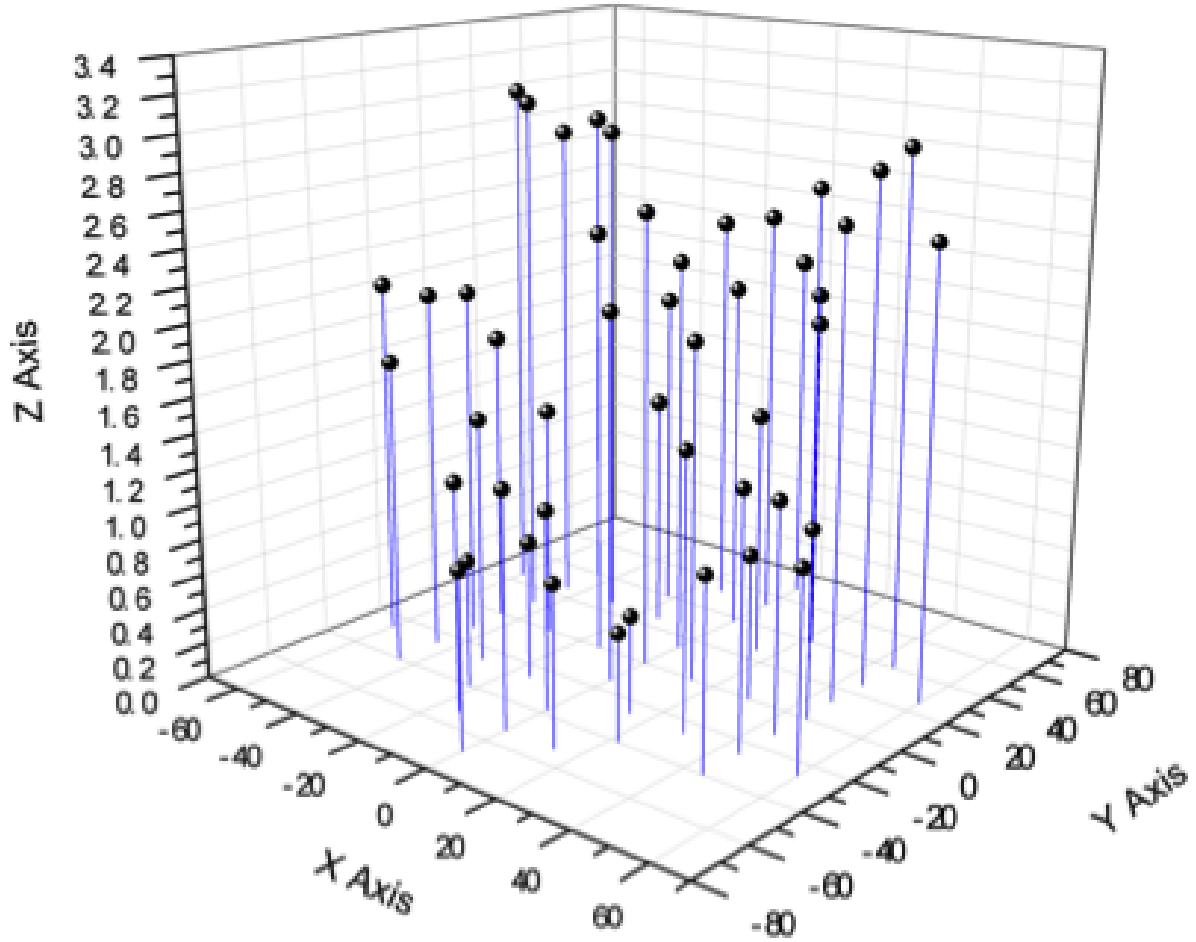


Figure 27: Induced voltage measurement result

## 5.0 CONCLUSIONS AND CONTRIBUTIONS

The experiments about a relayed WPT system showed that the relay resonator increased the power transfer distance of a magnetic resonant coupling WPT system and increased the efficiency. In a system with relay, the load value will affect the optimal relay position, so that the relay resonator should move toward the device resonator to achieve maximum efficiency. The load value will also affect the maximum efficiency. In the experimented cases, larger load value gave us higher efficiency. The multiple-resonator powering platform can supply over 0.5 V voltage regardless of the position on the wireless platform, which is enough in our application to rodent experiment with implanted devices. In addition, the innovative receiving resonator showed a high Q factor considering its small size.

### 5.1 CONTRIBUTIONS

In this thesis, we first derived the optimal condition for a three-resonator relayed magnetic resonant coupling WPT system to achieve the maximum efficiency using CMT, and performed experiments to verify our derivation. Then as an important application of multiple-resonator magnetic resonant coupling WPT system, we constructed a new platform for performing biological experiments on laboratory rodents implanted with miniature devices. Our WPT system supplies a sufficient amount energy to the implanted devices regardless of the locations of rodents in the platform. A new hexagonal PCB based resonator was designed. Seven such resonators were fabricated and placed under the platform in a unique pattern. These resonators transmit power to an innovative receiving resonator which is integrated within the container of an implanted device.

## 5.2 FUTURE WORK

A 50% efficiency is not enough for everyday use. Hence in the future, resonators with higher Q factors will be designed to achieve higher efficiency. These may require new material (e.g., superconductive material). More complex systems with even more resonators will need to be analyzed. And new parameter-measuring methods need to be tested to give more accurate measurements of the Q factor and coupling coefficients of the resonators, for example, Tetsuya et al presented their parameter-measuring method recently, where the parameters can be achieved using oscilloscope [30]. Also, a recent paper in Science introduced the idea of epidermal electronics, where magnetic resonant coupling WPT system can be integrated to supply power to electronic circuits for the measurement of some physiological signals [31]. Because the deformation of the tissue can change the resonant frequency of the epidermal resonator and thus change the behavior of the whole system, so by observing the feedback signal from the receiving resonator we may get the desired information. Theoretical analysis needs to be performed first to evaluate the signal-transmitting ability of a magnetic resonant coupling WPT system.

## BIBLIOGRAPHY

- [1] “Space solar power,” <http://www.brightgreencities.com/v1/en/bright-green-book/estados-unidos/energia-solar-espacial/>.
- [2] B. Gareth, “Win! a power mat wireless charging station for your iphone,” <http://www.techradar.com/news/world-of-tech/win-a-powermat-wireless-charging-station-for-your-iphone-717078>.
- [3] M. Jim, “Delphi and witricity developing wireless electric car charger,” <http://wheels.blogs.nytimes.com/2010/11/02/delphi-and-witricity-developing-wireless-electric-car-charger/>.
- [4] N. Tesla, “Apparatus for transmitting electrical energy,” U.S. Patent 1,119,732, 12, 1914.
- [5] J. B. William, “A battle to preserve a visionary’s bold failure,” <http://www.nytimes.com/2009/05/05/science/05tesla.html?pagewanted=all>.
- [6] P. E. Glaser, “Power from the sun: It’s future,” *Science*, vol. 162, pp. 867–886, 1968.
- [7] “Wireless electricity products spark a new industry,” <http://www.powerbeaminc.com/2010-05-07.php>.
- [8] G. Franceschetti, A. Massa, and P. Rocca, “Innovative antenna systems for efficient microwave power collection,” in *IMWS-IWPT2011 Proceedings*, 2011, pp. 13–14.
- [9] A. Karalis, J. D. Joannopoulos, and M. Soljačić, “Efficient wireless non-radiative mid-range energy transfer,” *Annals of Physics*, vol. 323, pp. 34–48, 2008.
- [10] J. Jackson, *Classical Electrodynamics*. Wiley: New York, 1999.
- [11] J. M. Fernandez and J. A. Borrás, “Contactless battery charger with wireless control link,” U.S. Patent 6,184,651, 02, 2001.
- [12] L. Ka-Lai, J. W. Hay, and P. G. W. Beart, “Contactless power transfer,” U.S. Patent 7,042,196, 05, 2006.

- [13] A. Kurs, A. Karalis, R. Moffatt, and et al, “Wireless power transfer via strongly coupled magnetic resonances,” *Science*, vol. 317, pp. 83–86, 2007.
- [14] L. C. Benjamin, F. H. James, and C. G. Seth, “Magnetic resonant coupling as a potential means for wireless power transfer to multiple small receivers,” *IEEE Transactions on Power Electronics*, vol. 24, pp. 1819–1825, 2009.
- [15] A. Kurs, R. Moffatt, and M. Soljačić, “Simultaneous mid-range power transfer to multiple devices,” *Applied Physics Letters*, vol. 96, pp. 044 102–044 103, 01 2010.
- [16] J. Kim, H. Son, D. Kim, K. Kim, and Y. Park, “Analysis of wireless energy transfer to multiple devices using cmt,” in *Microwave Conference Proceedings (AMPC), 2010 Asia-Pacific*, 2010, pp. 2149–2152.
- [17] A. P. Sample, D. A. Meyer, and S. J. R., “Analysis, experimental results and range adaptation of magnetically coupled resonators for wireless power transfer,” *IEEE Transactions on Industrial Electronics*, vol. 58, pp. 544–554, 02 2011.
- [18] H. Kim, S. Kang, S. Cheon, M. Lee, and T. Zyung, “Wireless power transmission to multi devices through resonant coupling,” in *International Conference on Electrical Machines and Systems (ICEMS)*, 2010, pp. 2000–2002.
- [19] T. C. Beh, T. Imura, M. Kato, and Y. Hori, “Basic study of improving efficiency of wireless power transfer via magnetic resonance coupling based on impedance matching,” in *IEEE International Symposium on Industrial Electronics*, 2010, pp. 2011–2016.
- [20] F. Zhang, S. A. Hackworth, W. Fu, and M. Sun, “The relay effect on wireless power transfer using witricity,” in *14th Biennial IEEE Conference on Electromagnetic Field Computation (CEFC)*, 05 2010, p. 1.
- [21] M. Dionigi and M. Mongiardo, “Efficiency investigations for wireless resonant energy links realized with resonant inductive coils,” in *German Microwave Conference*, 2011, pp. 1–4.
- [22] H. Hirayama, Y. Okuyama, and K. Kikuma, N. Sakakibara, “A consideration of equivalent circuit of magnetic-resonant wireless power transfer,” in *Proceedings of the 5th European Conference on Antennas and Propagation (EUCAP)*, 2011, pp. 900–903.
- [23] S. Shimokawa, H. Kawano, K. Matsui, A. Uchida, and M. Taguchi, “A numerical study of power loss factors in resonant magnetic coupling,” in *IMWS-IWPT2011 Proceedings*, 2011, pp. 219–222.
- [24] Y. Son, J. Kim, Y. Park, and K. Kim, “Efficiency analysis and optimal design of a circular loop resonant coil for wireless power transfer,” in *Asia-Pacific Microwave Conference Proceedings (APMC)*, 2010, pp. 849–852.

- [25] T. Imura and Y. Hori, “Maximizing air gap and efficiency of magnetic resonant coupling for wireless power transfer using equivalent circuit and neumann formula,” *IEEE Transactions on Industrial Electronics*, vol. 58, pp. 4746–4752, 2011.
- [26] H. A. Haus and W. Huang, “Coupled-mode theory,” in *Proceedings of IEEE*, vol. 79, 1991, pp. 1505–1518.
- [27] H. A. Haus, *Waves and fields in optoelectronics*. Prentice-Hall: New Jersey, 1984.
- [28] E. Roy and S. Philips, “Probing the magnetic field probe,” [http://www.compliance-club.com/archive/old\\_archive/030718.htm](http://www.compliance-club.com/archive/old_archive/030718.htm).
- [29] D. Kajfez, “Q factor measurements analog and digital,” [www.ee.olemiss.edu/darko/rfqmeas2b.pdf](http://www.ee.olemiss.edu/darko/rfqmeas2b.pdf).
- [30] T. Ishida, I. Awai, and I. Sugiyama, “Measurement of resonator parameters for wireless power transmission system,” in *IMWS-IWPT2011 Proceedings*, 2011, pp. 211–214.
- [31] D. Kim, N. Lu, R. Ma, and et al, “Epidermal electronics,” *Science*, vol. 333, no. 6044, pp. 838–843, 08 2011.